

LA-1157(Conf.)

LOS ALAMOS SCIENTIFIC LABORATORY
OF
THE UNIVERSITY OF CALIFORNIA

57722

May 22, 1950

This document consists of 62 pages

No. 13 of 20 copies, Series A

CLASSIFICATION CANCELLED
DATE <u>1-24-57</u>
For The Atomic Energy Commission
<u>H. P. Cansell</u>
Chief, Declassification Branch

ORALLOY HYDRIDE CRITICAL ASSEMBLIES

Work done by:

Group W-2

Report written by:

Part I : H. C. Paxton
Part II : J. D. Orndoff
Part III: G. A. Linenberger
Part IV : H. C. Paxton

Nuclear Components

~~SECRET~~

[Redacted]

[Redacted]

Washington Document Room
J. R. Oppenheimer
Los Alamos Document Room

1 thru 4
5
6 thru 20

~~SECRET~~

~~SECRET~~

ORALLOY HYDRIDE CRITICAL ASSEMBLIES

ABSTRACT

Part I of this report covers critical-mass determinations for pseudospheres of oralloy hydride composition (approximating UH_3) in 8"-thick Tu and Ni tampers and in the Tu tamper with Ni liner. The critical mass of a hydride cube in the thick Tu also is given. Data on weight and dimensional changes of hydride pieces during the period of use are included.

In Part II are presented the results of Rossi tire-scale measurements on the hydride assemblies. Values of alpha at delayed critical and its variation with mass in the neighborhood of delayed critical are given.

Measurements on the activation of various detectors within the hydride assemblies are described in Part III. Results as a function of radial position are given for Au, for Au shielded by Au and by Cd, for S and for fission catchers with U^{235} and U^{238} .

Reactivity changes resulting from the introduction of foreign materials into the hydride assemblies are discussed in Part IV. Apparent regularities with respect to Z and qualitative interpretations of variations with radius are pointed out. From data for various radial positions, changes in critical mass corresponding to small changes in composition and density are computed.

- 3 -
~~SECRET~~

~~SECRET~~

PART I

ORALLOY HYDRIDE CRITICAL ASSEMBLIES

CRITICAL SIZES IN THICK TU AND NI TAMPERS

Introduction

Assemblies of Oy H_{10} C_4 in various tampers were studied by Holloway and Baker⁽¹⁾ early in the history of The Los Alamos Scientific Laboratory.

It is hoped that com-

parisons between Oy and hydride systems, with their widely differing neutron spectra, may add insight into the behavior of reactive systems in general.

Hydride Composition

This report covers a series of measurements on critical assemblies of an oralloy hydride composition in thick Tu and Ni tampers. The hydride, a mixture of OyH_3 powder, Oy powder and polythene, was prepared in the desired shapes by the plastics section of Group CMR-6⁽³⁾. Examples of the shapes used are shown in Fig. I-1. The average empirical formula of the hydride composition is $UH_{2.93}C_{1.08}O_{0.26}$ with small deviations from part to part, and the mean piece density is 7.5 gm/cm^3 . Pseudospheres of hydride were assembled

⁽¹⁾Critical Masses of Enriched Uranium Hydrides and Some Related Measurements, M. G. Holloway and C. P. Baker, LA-1035 (12/19/47).

⁽²⁾Report on Hydride, S. Mosskowsky and D. Libermann, LA-1085 (May, 1950).

⁽³⁾Uranium Hydride Fabrication, Final Report, J. S. Church (in preparation).

~~SECRET~~

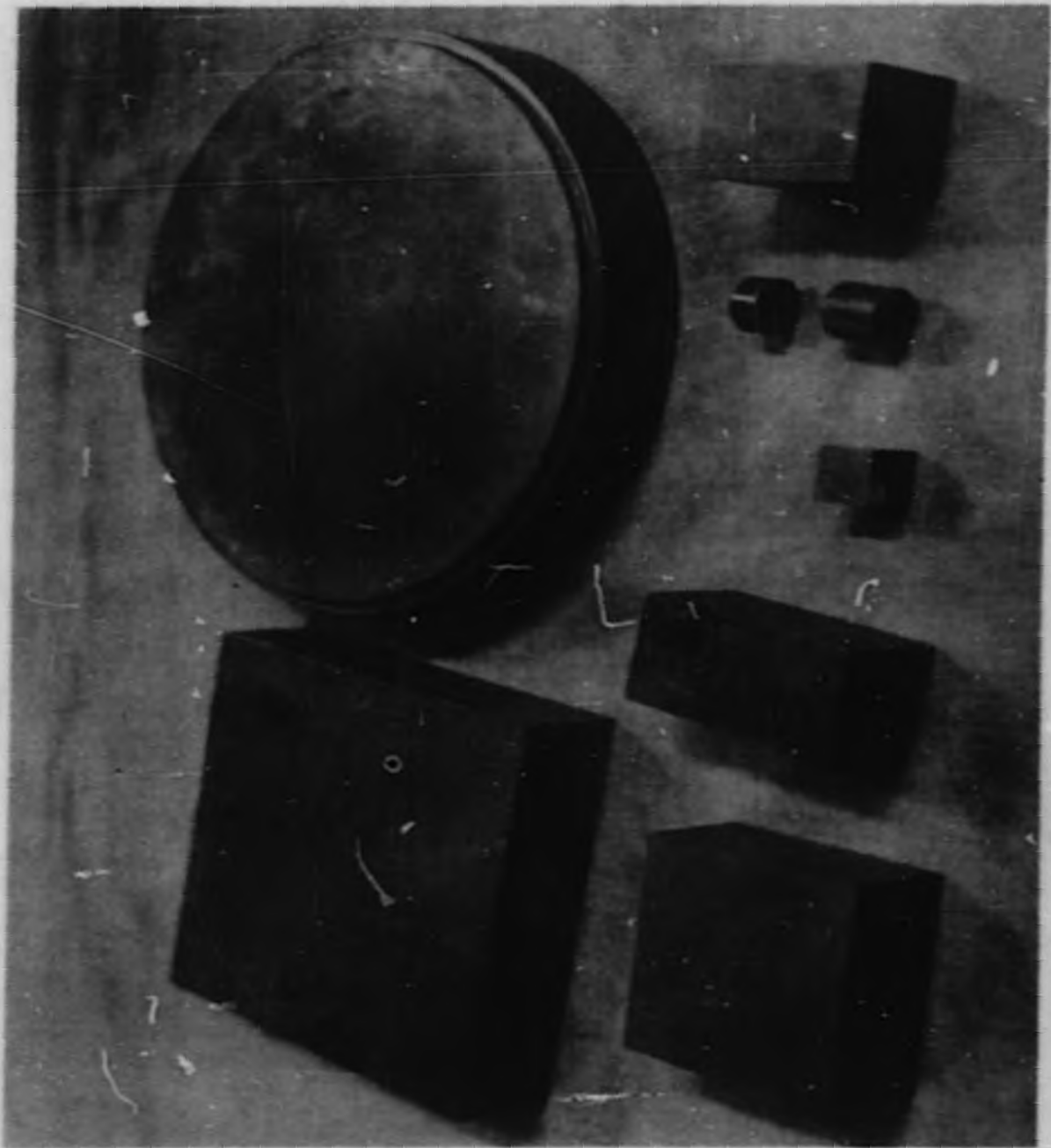
SECRET

FIG. I - 1
ORALLOY HYDRIDE SHAPES

- 5 -

SECRET

~~SECRET~~



- 6 -
~~SECRET~~

out of half-inch cubical units and surrounded by approximately 8"-thick tamper. A constant external tamper surface geometry was maintained for all measurements. The Tu tamper is effectively infinite, as was the case with an Oy metal core.

Assembly System

The hydride assemblies were set up on Topsy, the Pajarito universal machine for operation at delayed critical. A description of Topsy and of its use for measurements of the type to be discussed is given in LA-749.⁽⁴⁾ In brief, active material carried on the ram (A in Fig. I-2) may be moved by remote control into a cavity within a water tank (B) or into a cavity within a tamper mass (C). Neutron multiplication measurements⁽⁵⁾ in the water tank as a function of hydride mass establish the range of masses that may be stacked by hand in the ram with safety. The water is to simulate the tamping effect of a number of people near the ram; the multiplication limit for hand operations is 10. Once the safety of hand-stacking is established, multiplication measurements on successively larger pseudospheres of hydride raised into the tamper serve as a guide for the approach to delayed critical conditions.

Critical Size of Hydride in Tu Tamper

Results of the water-tank tests on hydride partially surrounded by Tu in the ram are given in Fig. I-3. Multiplication for the largest mass used

⁽⁴⁾ Polythene-25 Critical Assembly, H. C. Paxton and G. A. Linenberger, LA-749 (9/30/49)

⁽⁵⁾ Reference ("unmultiplied") counts were taken with tamper material substituted for the hydride. This led to conservative results, i.e., multiplication values in the water tank were slightly higher than with a polythene-Tu mockup of the hydride as reference configuration.

SECRET

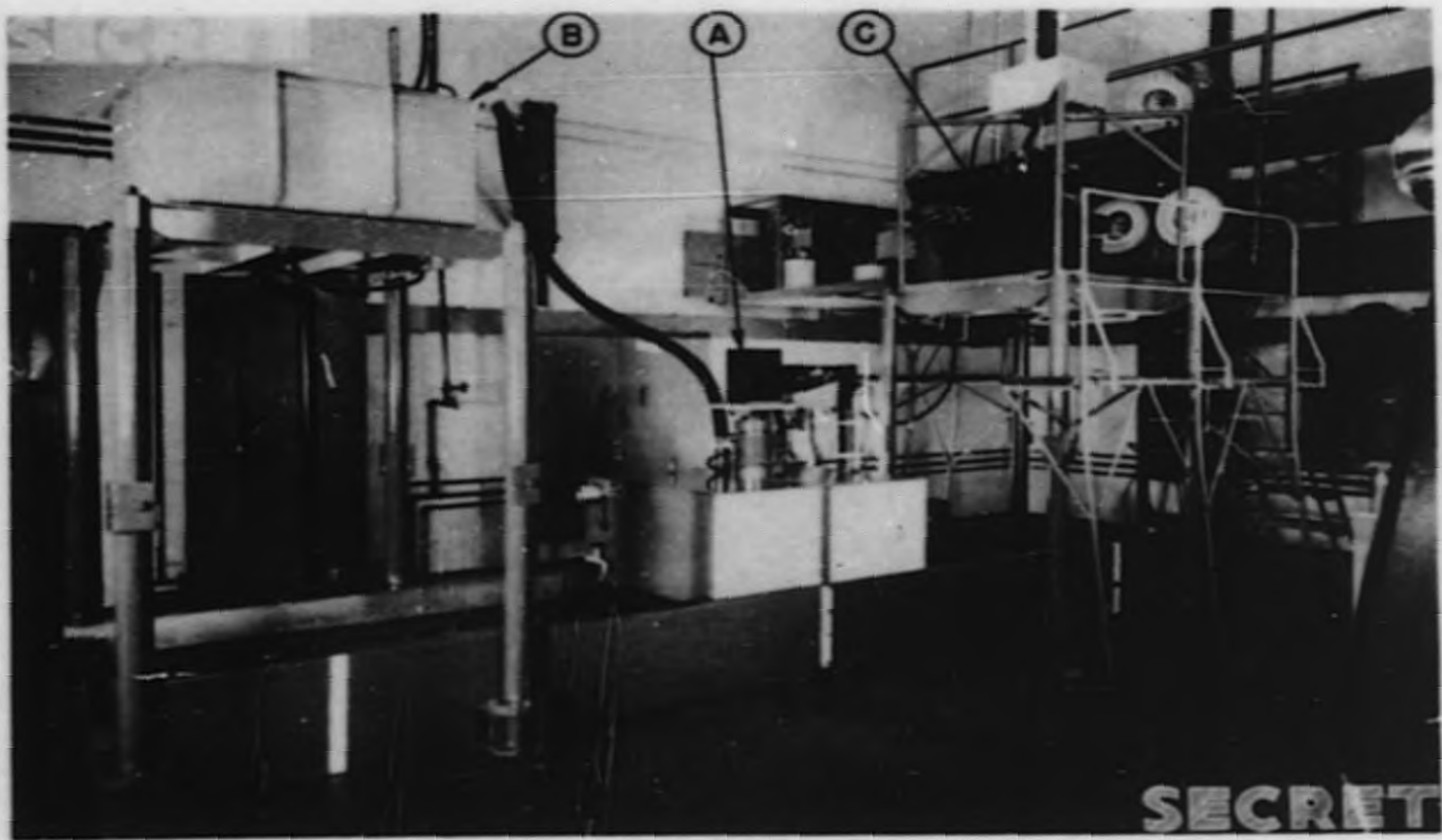
FIG. I - 2

TOPSY

- 8 -

SECRET

- 6 -



SECRET

SECRET

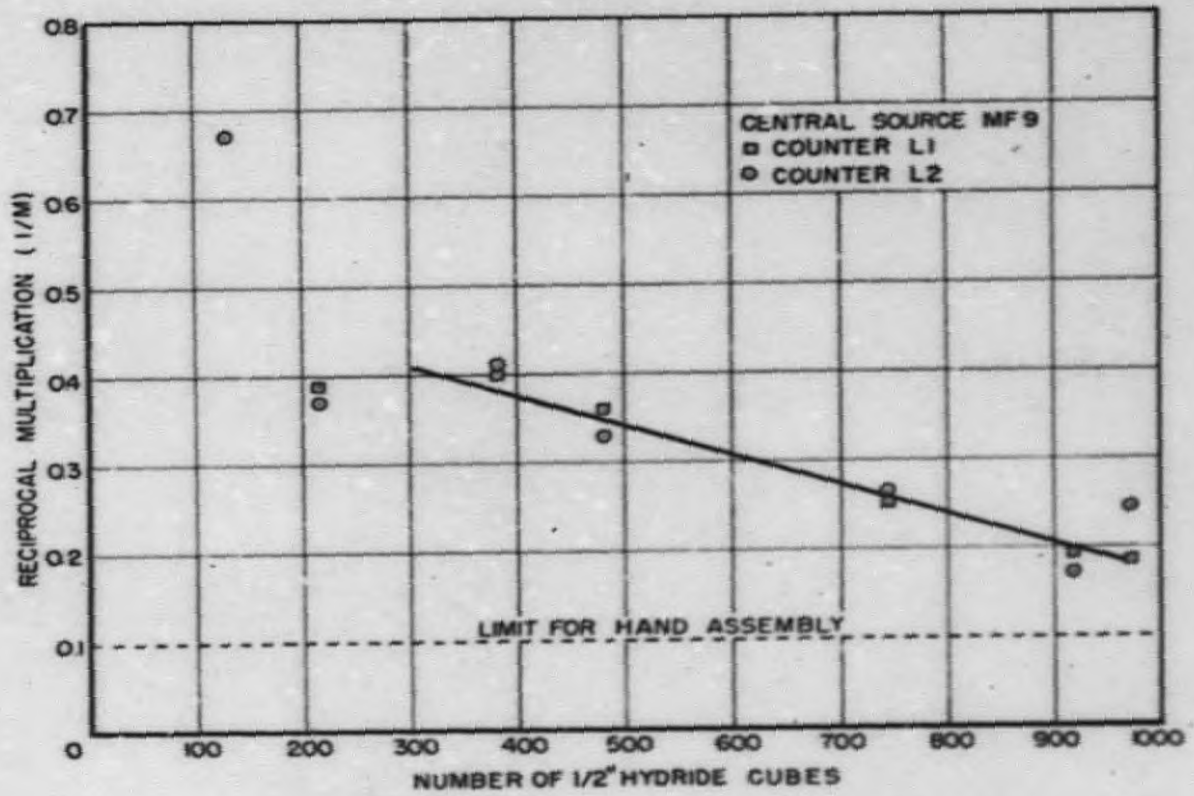


FIG. I-3. SAFETY TESTS - TOPSY WATER TANK
OF HYDRIDE WITH PARTIAL TU TAMPER

-10-

SECRET

S E C R E T

(14.7 kg) is about 5, i.e., well below the safety limit for hand-stacking. It may be remarked that hydride in the ram is less sensitive to surrounding water than is Qy metal (each of sufficient quantity to be critical in 8" Tu).

Measurements during the initial approach to delayed critical conditions in the thick Tu tamper are indicated in Fig. I-4. In this case, pseudospheres of hydride were imbedded in Tu on the ram. The critical quantity with both Topsy control rods "in" is seen to be equivalent of 967 half-inch cubes of hydride, or about 14.7 kg.

For neutron-distribution and time-scale measurements, it was necessary to set up a split hydride system as illustrated in Fig. I-5. The top pseudo-hemisphere, consisting of an hydride "stovelid" and additional pieces supported on it, is suspended within the tamper cavity, and the lower pseudo-hemisphere, nested in Tu, is carried on the ram. A radial hole (the "glory hole"), through the tamper and into the stovelid permits the use of internal measuring equipment which will not be disturbed by ram assembly. Fig. I-6 indicates results of a reapproach to critical with this split geometry. The critical volume, equivalent to 972 half-inch cubes (the critical mass again is 14.7 kg), is slightly higher than with all hydride in the ram because the stovelid density and H to U ratio were somewhat below the average for other pieces. The effect of each control rod is roughly that of 9 hydride cubes (134 gm hydride) in the outer portion of the pseudosphere.

SECRET

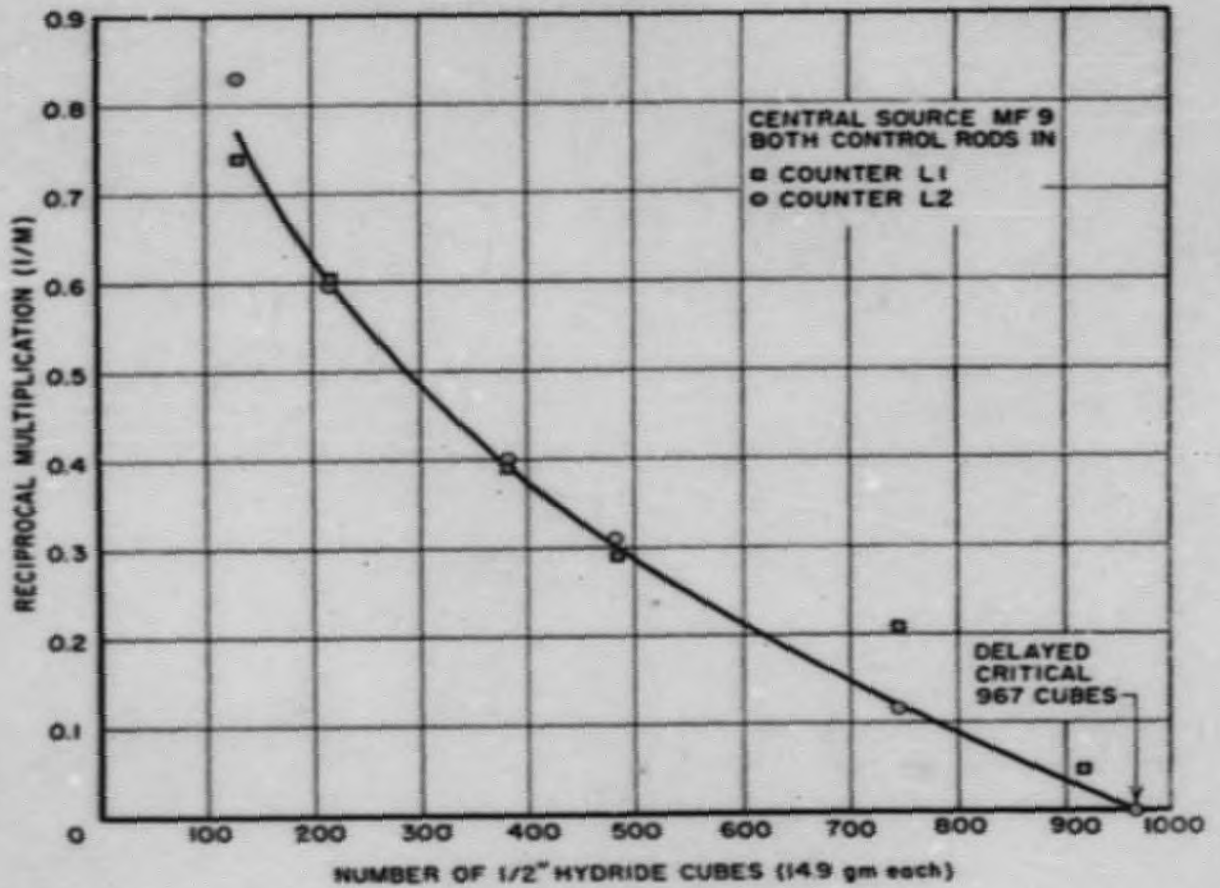


FIG. I-4. CRITICAL SIZE DETERMINATION
OF HYDRIDE IN 8" THICK TU TAMPER
PSEUDOSPHERE ON RAM

-12-

SECRET

SECRET

FIG. I - 5

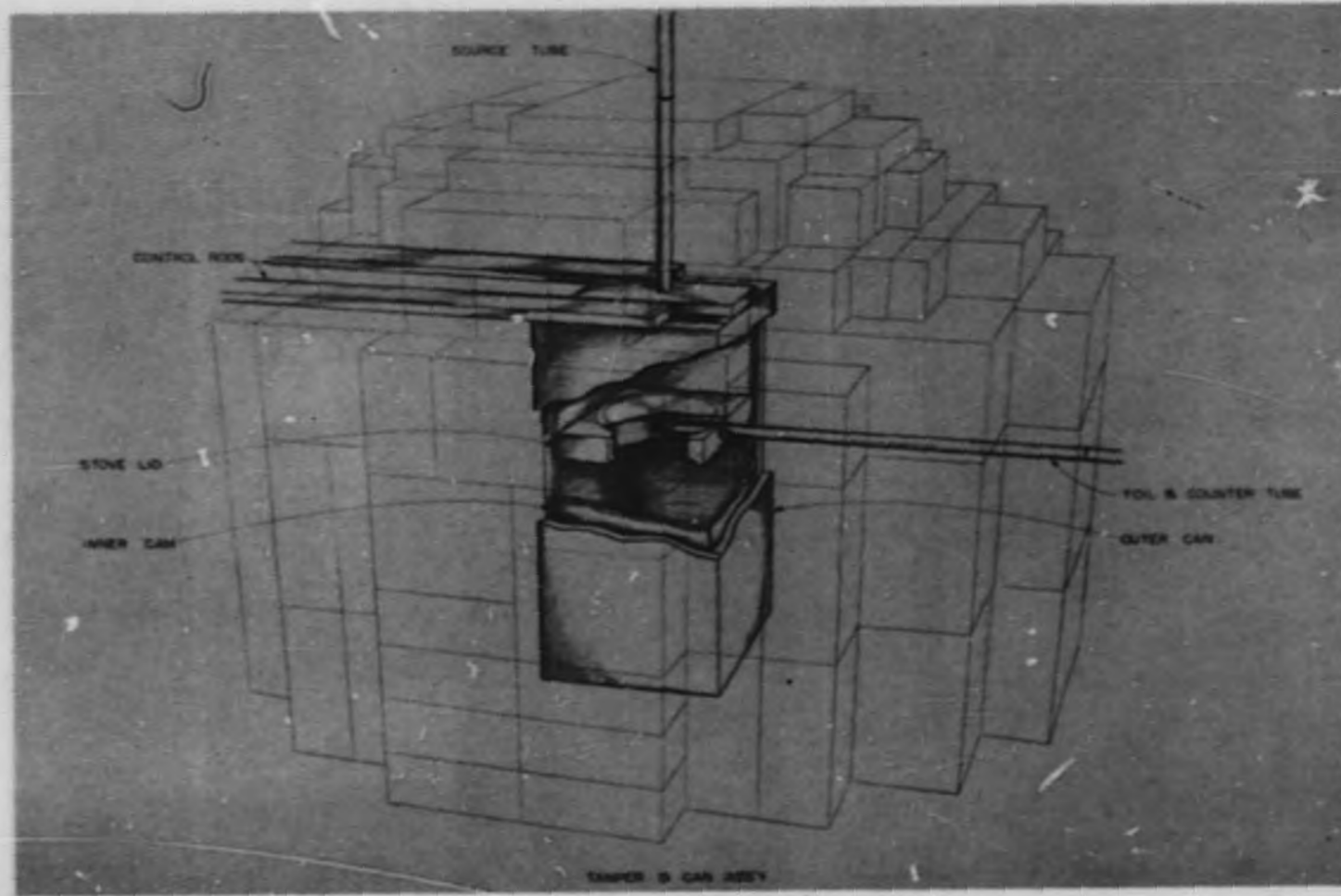
TOPSY SPLIT ASSEMBLY

The stovelid and Oy supported by it form the stationary upper half of the active core. The inner can, mounted on the ram, contains the lower half.

- 13 -

SECRET

SECRET
- 24 -



SECRET

SECRET

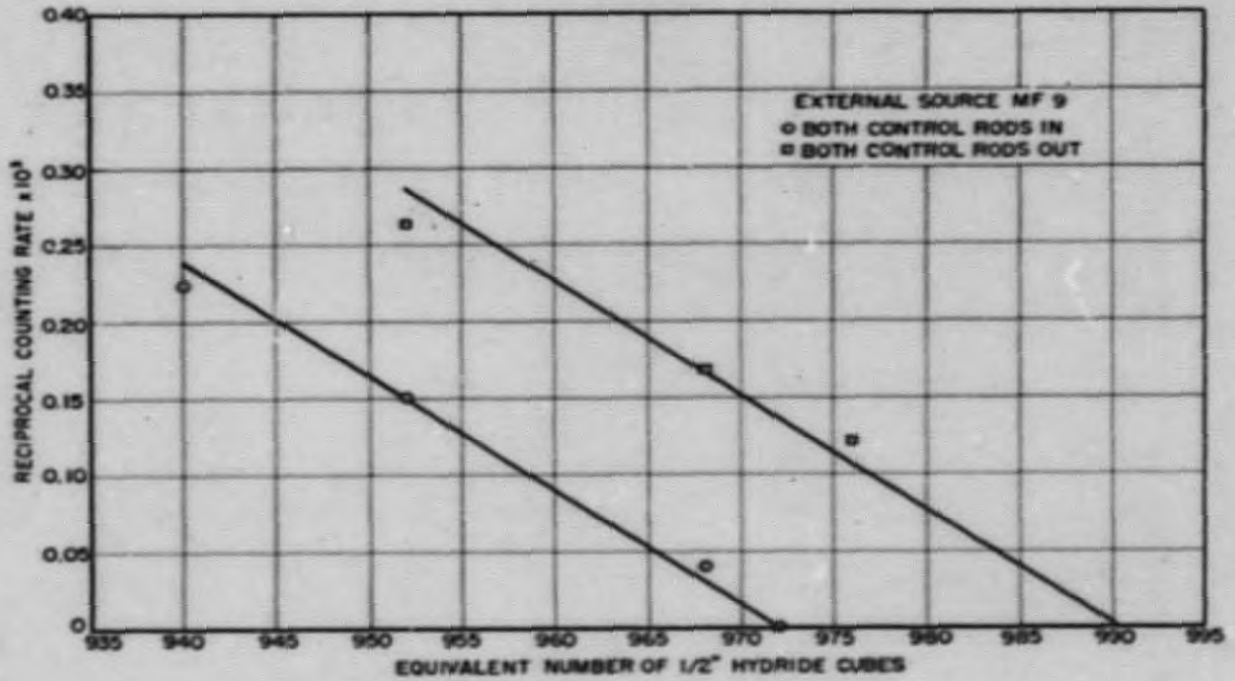


FIG 1-6. CRITICAL SIZE DETERMINATION
OF HYDRIDE IN 8" THICK TU TAMPER
SPLIT PSEUDOSPHERE

-5-

SECRET

SECRET

Data relevant to the delayed critical assemblies are summarized in the following table.

TABLE I-1

<u>HYDRIDE IN TU</u>	<u>ON RAM</u>	<u>SPLIT</u>
Avg. Empirical Formula	$\text{UH}_{2.97}\text{C}_{1.11}\text{O}_{0.25}$	$\text{UH}_{2.92}\text{C}_{1.08}\text{O}_{0.26}$
Critical Mass	14.68 kg	14.68 kg
Oy Content of Critical Mass	13.54 kg	13.55 kg
Concentration of U^{235} in Oy	93.15 %	93.15 %
Effective Hydride Density	7.40 gm/cm ³	7.35 gm/cm ³
Critical Volume	120.9 in. ³ 1980 cm ³	121.5 in. ³ 1990 cm ³
Radius of Sphere of Critical Volume	3.06"	3.07 cm"

TU TAMPER

Tu Thickness at Glory Hole	8"
Tu Mass	2550 kg
Tu Density	19 gm/cm ³

The above figures were obtained during the initial phase of hydride tests. About four months after the original stacking, the critical mass of the Tu-tamped hydride apparently had increased on the order of 1%. It is possible that a tamper change in this interval may be responsible for the effect.

It may be noted that results of Holloway and Baker correspond to a critical mass of 6.8 kg for $\text{Oy}(93\%) \text{H}_{10}$ of density 3.05 gm/cm³ in a 6½"-thick Tu tamper, or a critical volume of 2230 cm³.

S E C R E T

Critical Size of Hydride in Ni Tamper

For hydride partially tamped by Ni (stacked on the ram) the water-tank tests again indicated no hand-stacking restriction for the largest mass required (Fig. I-7). Fig. I-8 gives data for the approach to critical in the thick Ni tamper with all hydride on the ram, and similar data for the split assembly are shown in Fig. I-9. The critical quantities of hydride, 970 cubes (14.7 kg) and 976 equivalent cubes, respectively, are nearly identical with values for the Tu tamper. The effect per control rod is seen to be the equivalent of about 7 cubes, (104 gm hydride).

Table I-2 is a summary of data for these critical configurations.

TABLE I-2

<u>HYDRIDE IN NI</u>	<u>ON RAM</u>	<u>SPLIT</u>
Avg. Empirical Formula	$UH_{2.97}C_{1.11}O_{0.25}$	$UH_{2.92}C_{1.08}O_{0.26}$
Critical Mass	14.72 kg	14.74 kg
Oy Content of Critical Mass	13.56 kg	13.60 kg
Concentration of U^{235} in Oy	93.15 %	93.15 %
Effective Hydride Density	7.40 gm/cm ³	7.35 gm/cm ³
Critical Volume	121.2 in ³ 1990 cm ³	122.0 in ³ 2000 cm ³
Radius of Sphere of Critical Volume	3.07"	3.08"

NI TAMPER

Ni Thickness at Glory Hole	8"
Ni Mass	1180 kg
Ni Density	8.8 gm/cm ³

SECRET

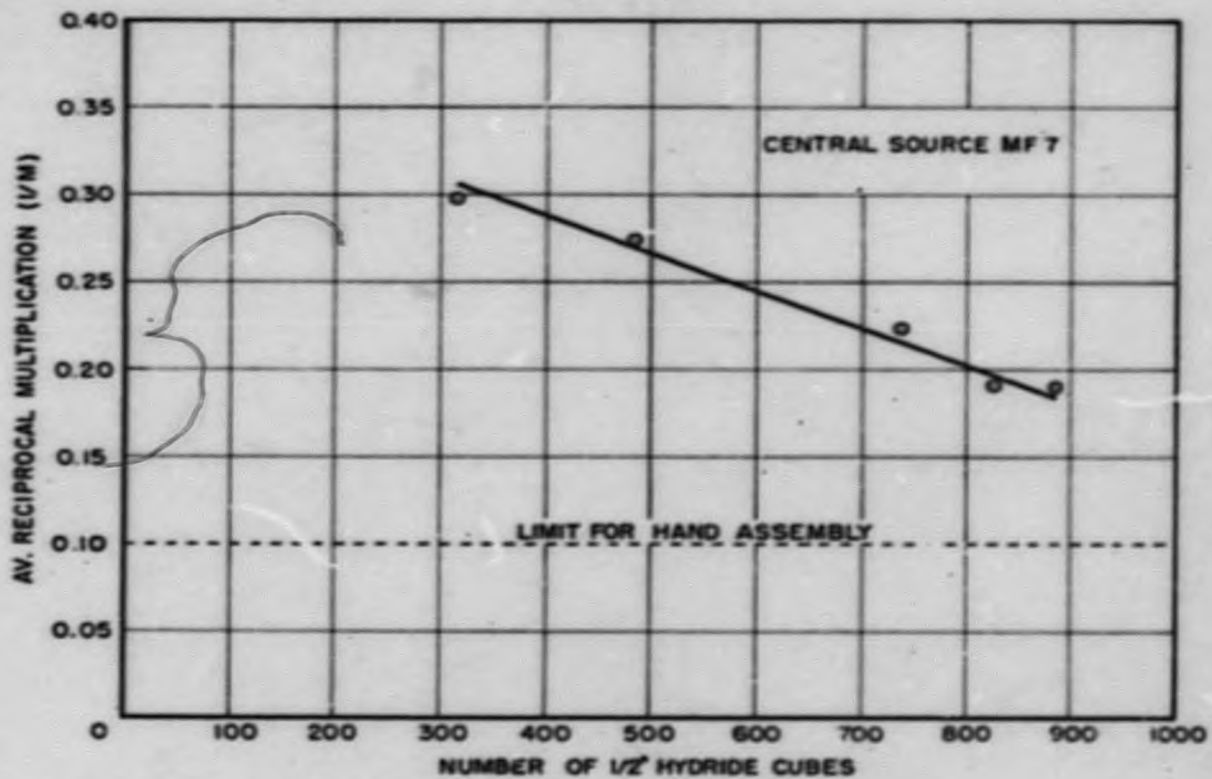


FIG. I-7. SAFETY TESTS - TOPSY WATER TANK
BY HYDRIDE WITH PARTIAL NI TAMPER

-18-

SECRET

SECRET

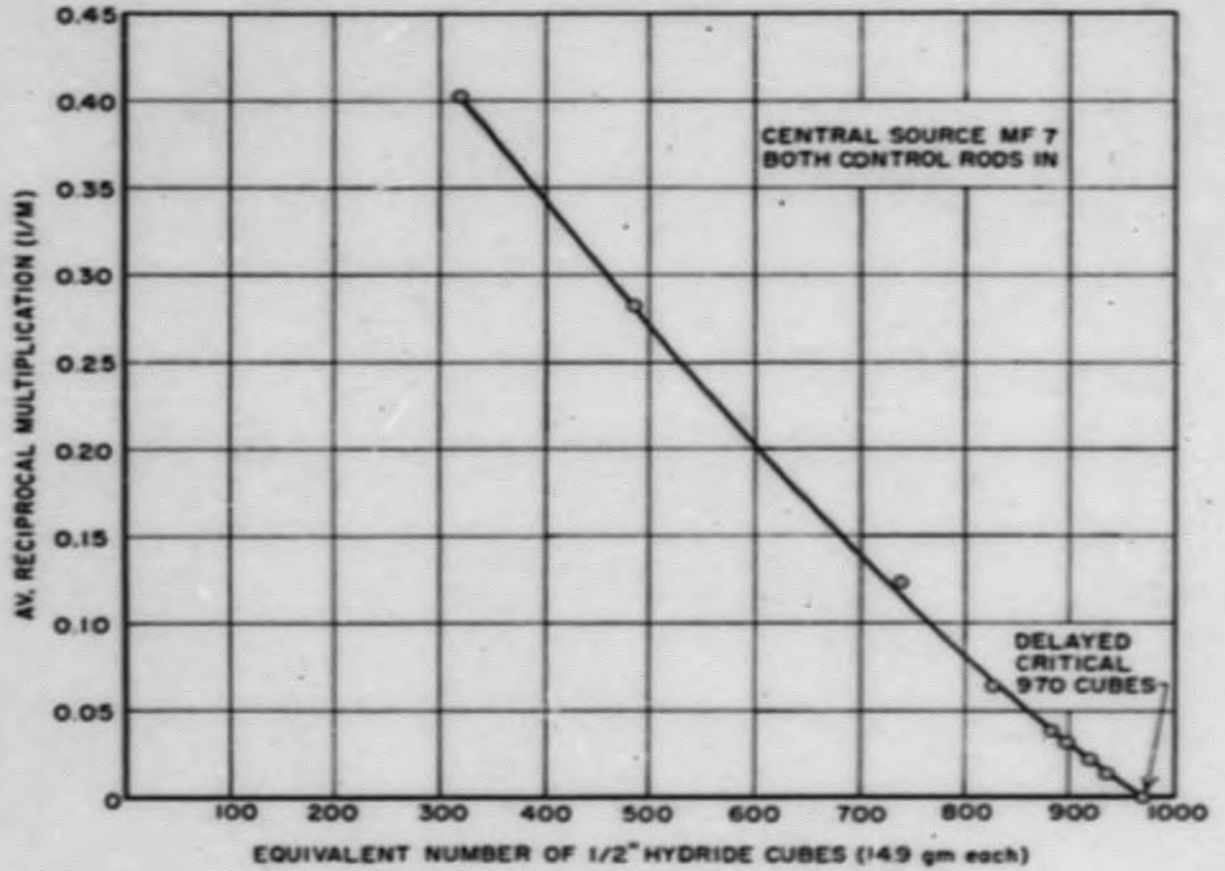


FIG. I-8. CRITICAL SIZE DETERMINATION
OF HYDRIDE IN 8" THICK Ni TAMPER
PSEUDOSPHERE ON RAM

-19-

SECRET

SECRET

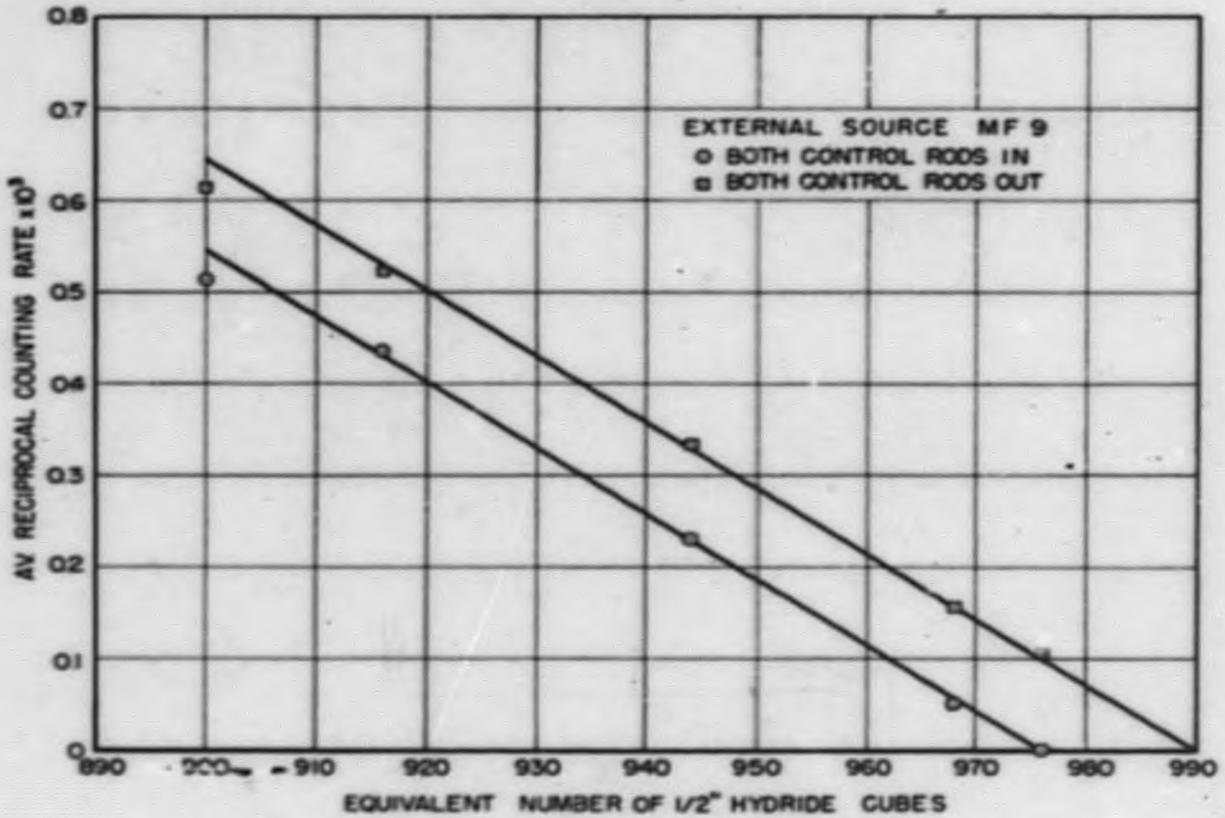


FIG. I-9. CRITICAL SIZE DETERMINATION
OF HYDRIDE IN 8" THICK NI TAMPER
SPLIT PSEUDOSPHERE

-20-

SECRET

S E C R E T

Shape Factor

As a guide to the influence of shape variation on reactivity, the critical mass of a hydride pseudocube in the thick Tu tamper was measured. The form was a 5" cube with 1/2" x 1/2" columns lacking along 4 parallel edges (a limitation imposed by Topsy design). To build up the required size, 35 additional half-inch cubes were placed in three groups on separate faces. The critical quantity was equivalent to 995 half-inch cubes as compared with 967 for a pseudosphere. The corresponding shape factor of 0.971 for pseudocube relative to pseudosphere agrees with that determined for Gy metal in thick Tu (0.968 for approximate cube relative to pseudosphere).

Composite Tamper

Material-replacement measurements (see Part IV) showed that substitution of Ni for a half-inch Tu cube adjoining the hydride core increases the reactivity of the system, whether in Tu or Ni tamper. Since critical masses in thick Tu and Ni tampers were essentially equal, this suggests that a composite tamper consisting of a relatively thin Ni layer about the hydride, surrounded in turn by thick Tu, should lead to a reduction in critical mass. According to a computation based on material replacement data, this decrease in critical mass should be 10% for a uniform half-inch Ni liner in a thick Tu tamper.

Accordingly, final hydride tests consisted of critical-mass determinations with one-inch and with half-inch Ni liners (roughly approximated) in the Tu tamper. The liners were imperfect because of Topsy design limitation; e.g., the approximately one-inch Ni layer thinned to 1/2" at a few locations about the equator of the pseudosphere and extended into the Tu in other places, and there were a few gaps and 1/4"-thick regions in the approximately half-inch layer.

S E C R E T

With the 1" Ni-lined Tu tamper, the critical quantity of hydride was equivalent to 905 half-inch cubes as compared with about 980 cubes for the final critical condition in unlined Tu. This amounts to a 7- $\frac{1}{2}$ % decrease in critical mass. The assembly with the half-inch Ni liner was critical at the equivalent of 918 cubes or about 6- $\frac{1}{2}$ % below the value for thick Tu. The latter difference might be expected to increase to about 8% or 9% if deficiencies in the half-inch Ni layer were removed. Although it is apparent that the observed magnitudes are open to question because of geometrical compromises, the expected effect appears to have been established.

Hydride Stability

The hydride was set up in Topsy for five and one-half months. During this time, weights and dimensions of six half-inch cubes and one 1" x 1" x 2" piece of hydride were checked periodically. The percent changes for individual pieces are given in Figs. I-10 and I-11. The weight gain in five and one-half months averaged 0.085% for the half-inch cubes and was 0.04% for the 1" x 1" x 2" block, and the average increase in linear dimensions was 0.2% for the half-inch cubes and 0.07% for the larger piece. The nearly constant rate indicated in Fig. I-10 is considered more reliable than the apparently decreasing rate of Fig. I-11 -- a zero error of 0.0005" could account for the knee apparently formed by the 54-day points in the latter group of curves.

SECRET

-23-

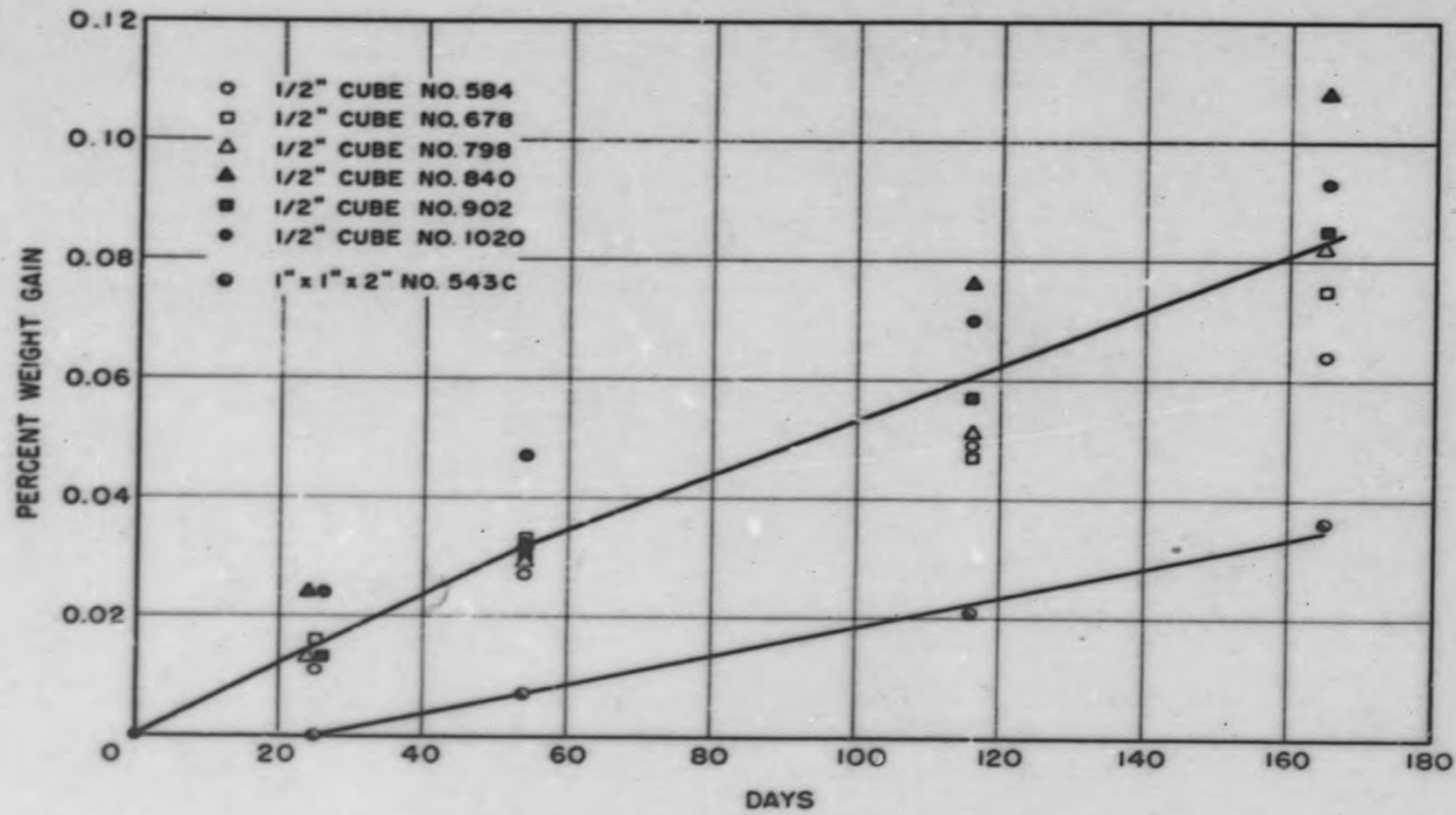


FIG. I-10 WEIGHT GAIN OF HYDRIDE SAMPLES DURING CRITICAL TESTS

SECRET

SECRET

-24-

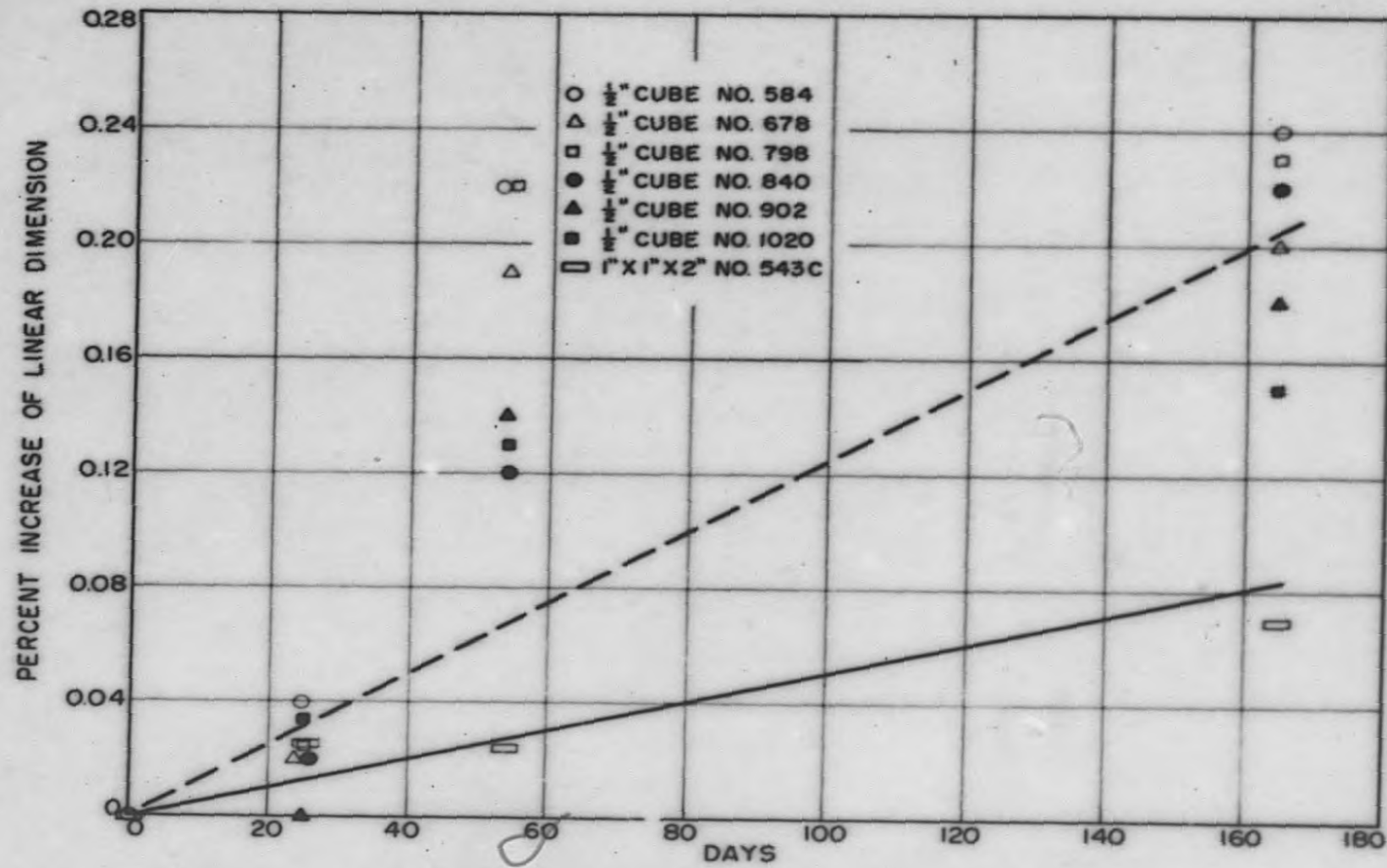


FIG. I-II DIMENSIONAL INCREASE OF HYDRIDE SAMPLES DURING CRITICAL TESTS

SECRET

S E C R E T

PART II

TIME-SCALE MEASUREMENTS ON HYDRIDE ASSEMBLIES

The general procedures for making measurements of α_c by the Rossi method on near-critical assemblies have been described in LA-744⁽¹⁾. The apparatus used consisted of (1) detector, (2) amplifier-discriminator and (3) time analyzer.

The neutron detectors employed were U^{235} spiral fission chambers. These chambers were approximately 7/8 inch in diameter and fit snugly into the 7/8-inch "glory hole" in the tamper. Since the glory hole in the hydride core was only half-inch in diameter, the detectors were inserted up to the tamper-hydride interface; this resulted in a minimum perturbation of the assembly. The foils in the spiral chambers contained 2 milligrams of U^{235} per cm^2 (~ 0.45 gm total). These thick foils did not give a pulse-height plateau, but did give a high efficiency. In operation, the discriminators were set low enough that a few alpha background pulses were recorded.

The new model 502 pulse amplifiers were used and have proved to be superior to the previously used model 501 amplifiers. Output pulses were about 0.5 microseconds total width. Very little trouble was experienced with these amplifiers "ringing", and they are much superior to the old amplifiers in this respect. The amplifiers fed into a special high-speed discriminator which drove the 1200 feet of cable terminated in 75 ohms. The final pulse input to the time scale apparatus consisted of square, equal height pulses 0.3 microseconds wide and 18 volts high. There was very little straggling of

⁽¹⁾ Time Scale Measurements by the Rossi Method, J. Orndoff and C. Johnstone, LA-744 (Nov. 9, 1949).

S E C R E T

pulse heights. The over-all counting system was quite stable. The system was operated at extreme gain and did pick up some noise pulses when the Topsy controls were operated. This noise background was not objectionable since it was not necessary to touch the controls during a Rossi run except for some slight control rod adjustments.

The time analyzer has been described in great detail in LA-744, consequently it will not be discussed in this report. The 3 microsecond channels proved to be the optimum width for all the hydride measurements. A few check measurements were made using 10 microsecond channel widths.

Measurements were made of α at critical and at various subcritical points. The subcritical points were obtained by stacking up to critical and then removing cubes in the required steps. The steps used were minus 4, 8, 12 and 16 half-inch hydride cubes. The cubes were removed from the outside of the hydride pseudosphere in such a fashion that they were representative of an outside layer of material. The mass increments removed, Δm , presumably produced equal increments of change in the reactivity, ΔK . No attempt was made to evaluate the K at different values of reactivity.

Fig. II-1 shows a plot of the α determinations on the tuballoy tamped hydride assembly. The P_c plotted is the probability after receiving a count, of receiving a second count originating from the same chain after a time, t , within the interval of time, Δt , equal to a channel width. It has been shown that these coincidences have the time dependence $e^{-\alpha t}$ so that alpha is determined from the slopes of the curves. The mean errors indicated on the last points are the maximum encountered, as statistics are much better for the earlier channels.

The same data for the nickel tamped assembly is collected in Fig. II-2. The series of experiments with the two different tampers were identical in all respects. The tamper stacking was the standard 8 inch tamper and all details

SECRET

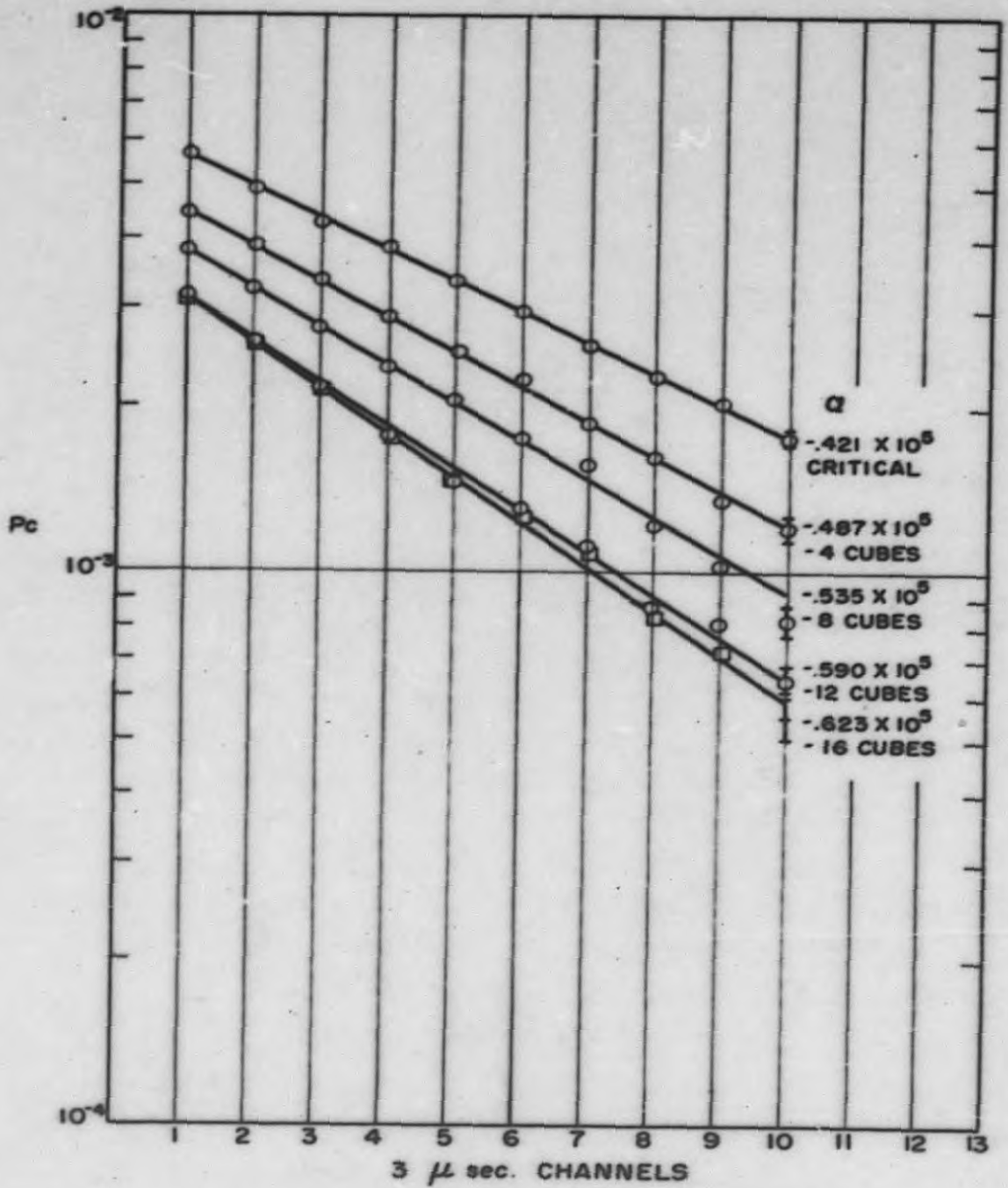


FIG. II - 1 AVERAGE HYDRIDE - TUBALLOY
ROSSI MEASUREMENTS

-27-

SECRET

SECRET

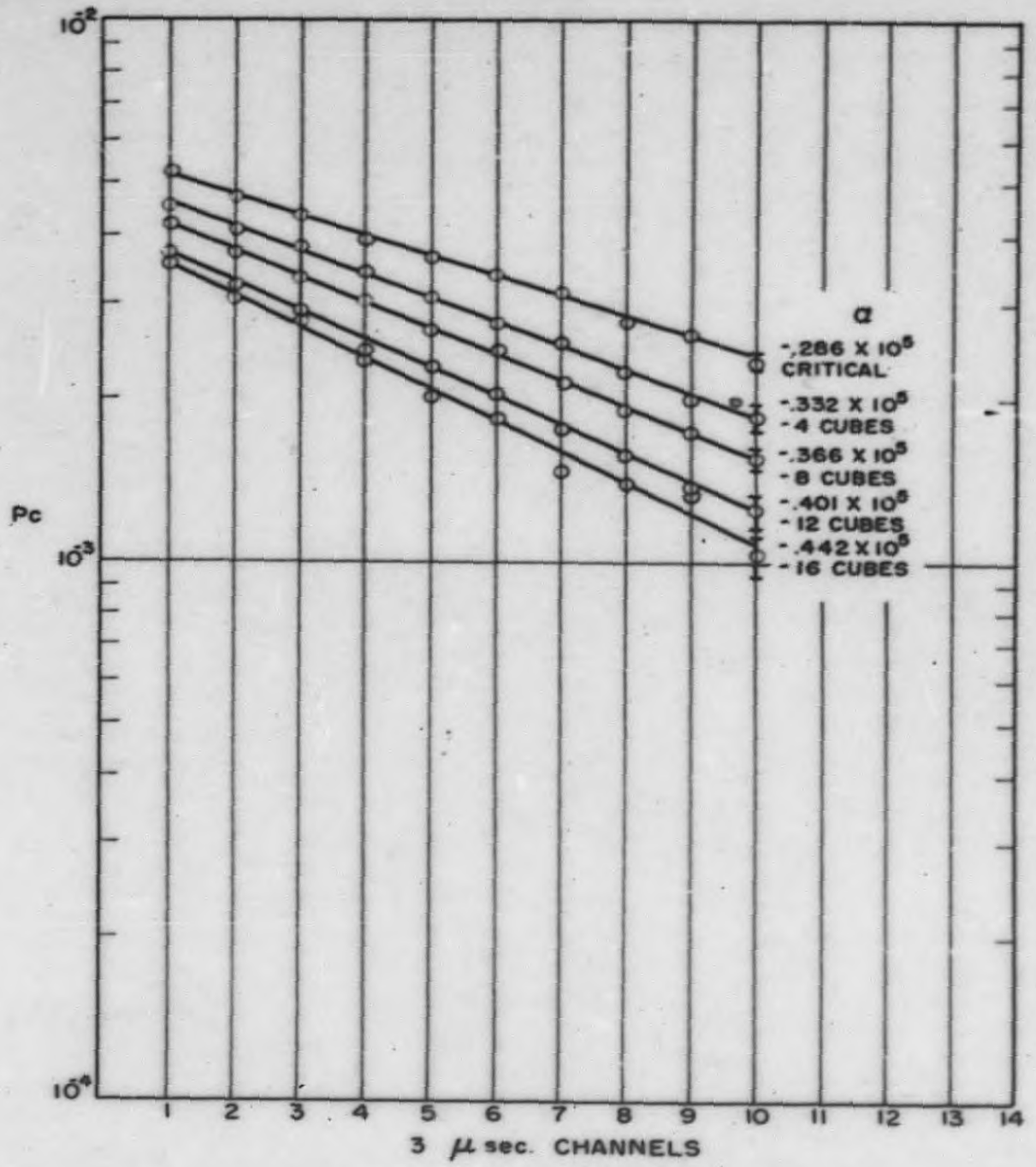


FIG. II-2 AVERAGE HYDRIDE-NICKEL
ROSSI MEASUREMENTS
-28-

SECRET

S E C R E T

of the tuballoy system including the inner and outer cans, the can on the ram and the tamper itself were faithfully reproduced in the nickel tamper. As it happened, the critical masses also were practically identical. A summary of all the data is given in the table below (Table II-1).

TABLE II-1
TUBALLOY TAMPER

Δm (gm)	$-\alpha$ (sec ⁻¹)	τ_0 (sec)
0	0.421×10^5	1.8×10^{-7}
-59.6	0.487×10^5	
-119	0.535×10^5	
-179	0.590×10^5	
-238	0.623×10^5	

NICKEL TAMPER

Δm (gm)	$-\alpha$ (sec ⁻¹)	τ_0 (sec)
0	0.286×10^5	2.7×10^{-7}
-59.6	0.332×10^5	
-119	0.366×10^5	
-179	0.401×10^5	
-238	0.442×10^5	

The value of τ_0 , the mean life of a neutron in the assembly, was obtained from the relation

$$\alpha = \frac{K_p - 1}{\tau_0}$$

where K_p is the average number of prompt daughter neutrons per neutron. At delayed critical, the value of $K_p - 1$ was taken to be .0076 which is equal to the fraction of neutrons that are delayed. This will be true only if the

S E C R E T

effectiveness of delayed neutrons for producing fissions is the same as that for prompt neutrons. Such an assumption may not be justified. If delayed neutrons are more effective for producing fissions than prompt neutrons, the value of λ_d quoted will be too low.

In order to compare the values of α measured for the present hydride assembly with values for other assemblies, the results of some previous measurements are listed in the table below.

TABLE II-2

ACTIVE MATERIAL	TAMPER	REACTIVITY LEVEL	$-\alpha \text{ SEC}^{-1}$	REFERENCE
Oy	Tu	Critical	0.37×10^6	LA-744
UH ₁₀	BeO	Approx. Crit.	0.18×10^4	LA-1035
UH ₁₀	WC	Approx. Crit.	0.79×10^4	LA-1035

The variation of α with mass is plotted in Fig. II-3 for both tampers. These curves give values of $d\alpha/dm$ equal to $0.93 \times 10^2 \text{ sec}^{-1} \text{ gm}^{-1}$ for the tuballoy tamper and $0.66 \times 10^2 \text{ sec}^{-1} \text{ gm}^{-1}$ for the nickel tamper. The differences observed in α and in $d\alpha/dm$ can be interpreted as being due to tamper alone since the cores in the two cases were identical.

A progressive increase of α over a period of months was observed with the hydride assembly. The increase was sufficiently large that any possibility of accounting for it on the basis of experimental uncertainties must be discounted. A graph of the time variation of α is given in Fig. II-4. The uncertainties ascribed to the points are considered to be the maximum experimental uncertainties. Weights and sizes of hydride cubes did not change

D

SECRET

β^{-31}

SECRET

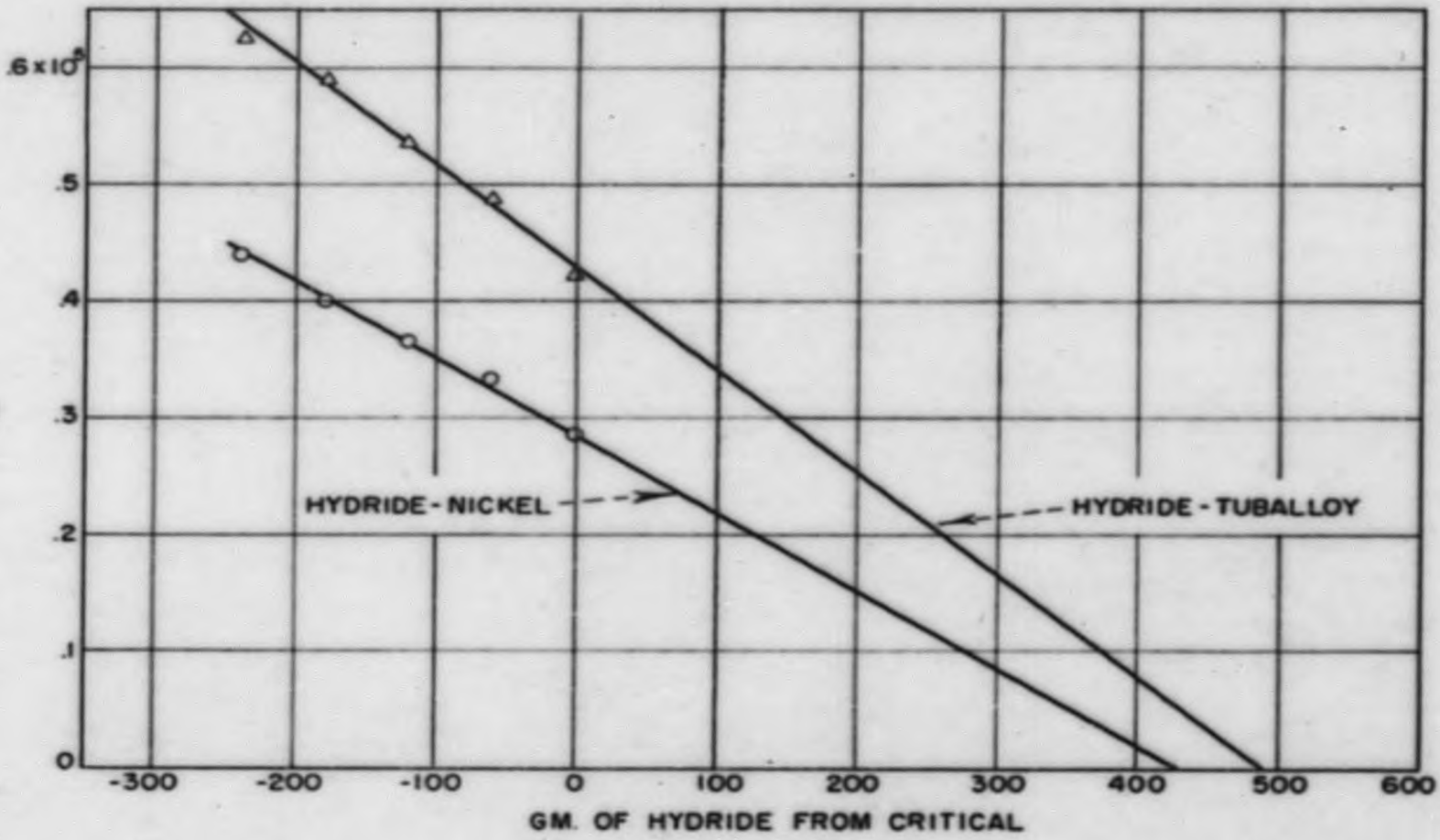


FIG. II-3 ROSSI DATA

SECRET

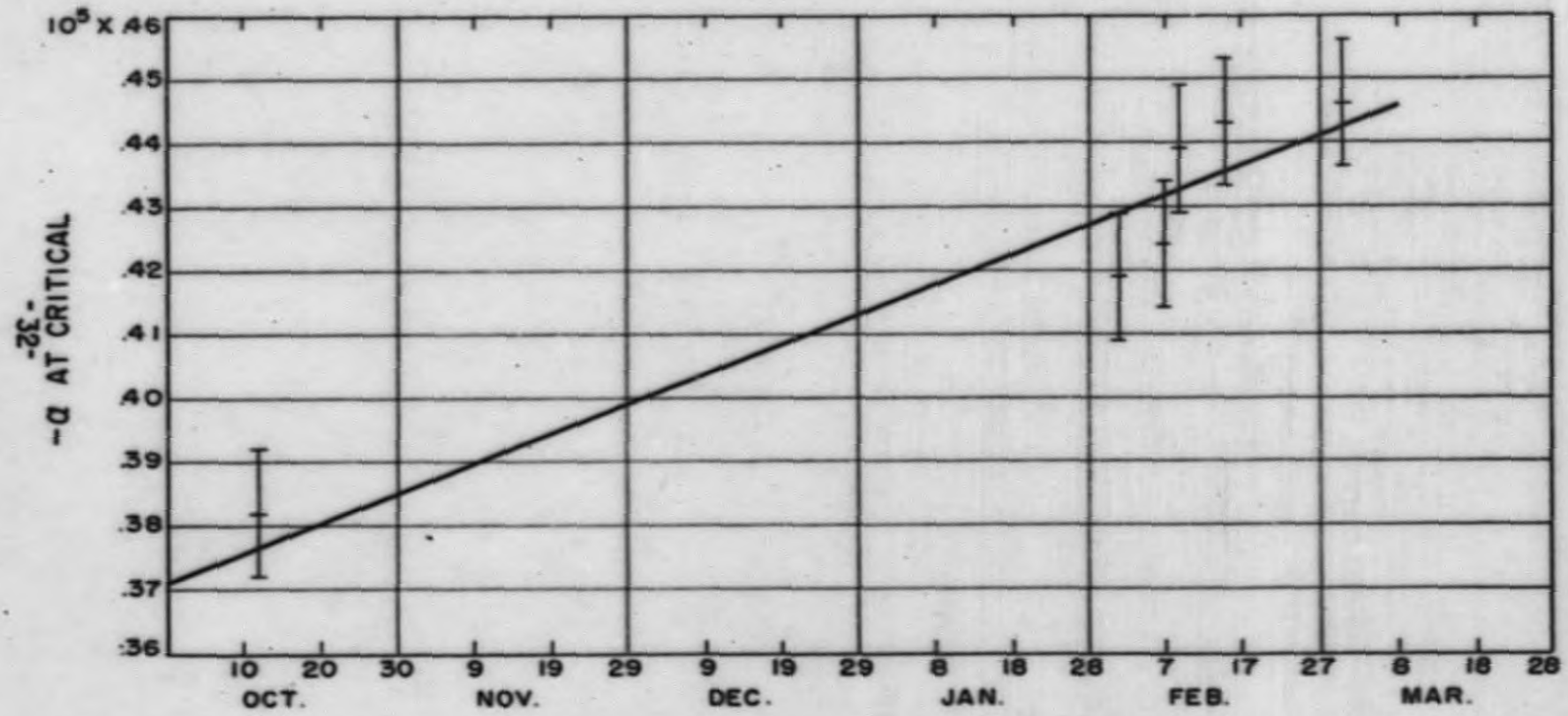


FIG. II-4 VARIATION OF α WITH TIME FOR HYDRIDE-TUBALLOY

SECRET

S E C R E T

appreciably during the period (Part I). There is the possibility that the plastics in the hydride mixture decomposed with loss of hydrogen under the influence of ionizing radiation.

The Rossi measurements reported for the tuballoy and nickel taspers were done within about one month of each other. The "age" effect on α might have changed α by a few percent during this interval of time.

S E C R E T

PART III

NEUTRON DISTRIBUTION STUDIES

The methods used in making these measurements have been described in detail in LA-749, which deals with the mock-hydride reactor, the only difference being that all beta activity measurements for the present report were made with methane-flow proportional counters calibrated for each type of detector used.

Detectors of gold, sulphur, or alloy (containing 94% U^{235}), and U^{238} (ratio of U^{238} to U^{235} is about five thousand to one) were used, the reactions of interest being (n, γ) for the gold, (n, p) for the sulphur (effective threshold ca. 3 Mev), and fission for U^{235} and U^{238} . Both the gold and the sulphur were in the form of 0.49" diameter foils, the gold being 5 mils thick and the sulphur about 0.12" thick (0.60 gm. pressed into a pellet). The U^{238} and alloy were in the form of 1 mil foils 0.44" diameter, and were irradiated in contact with 10 mil celluloid fragment catcher foils of the same diameter. These detectors were distributed at various radii throughout the hydride and tamper, and were irradiated by running the reactor at delayed critical.

The results are presented graphically in Figs. III-1 through III-5, for which the total number of disintegrations per atom of detector (for standard irradiation conditions) is plotted against position of detector in the assembly. Irradiations were standardized by monitoring with a sulphur pellet placed at the center of the reactor during each irradiation. Fig. III-6 gives the ratio of the fission rate of U^{238} to that of alloy as a function of radius.

SECRET

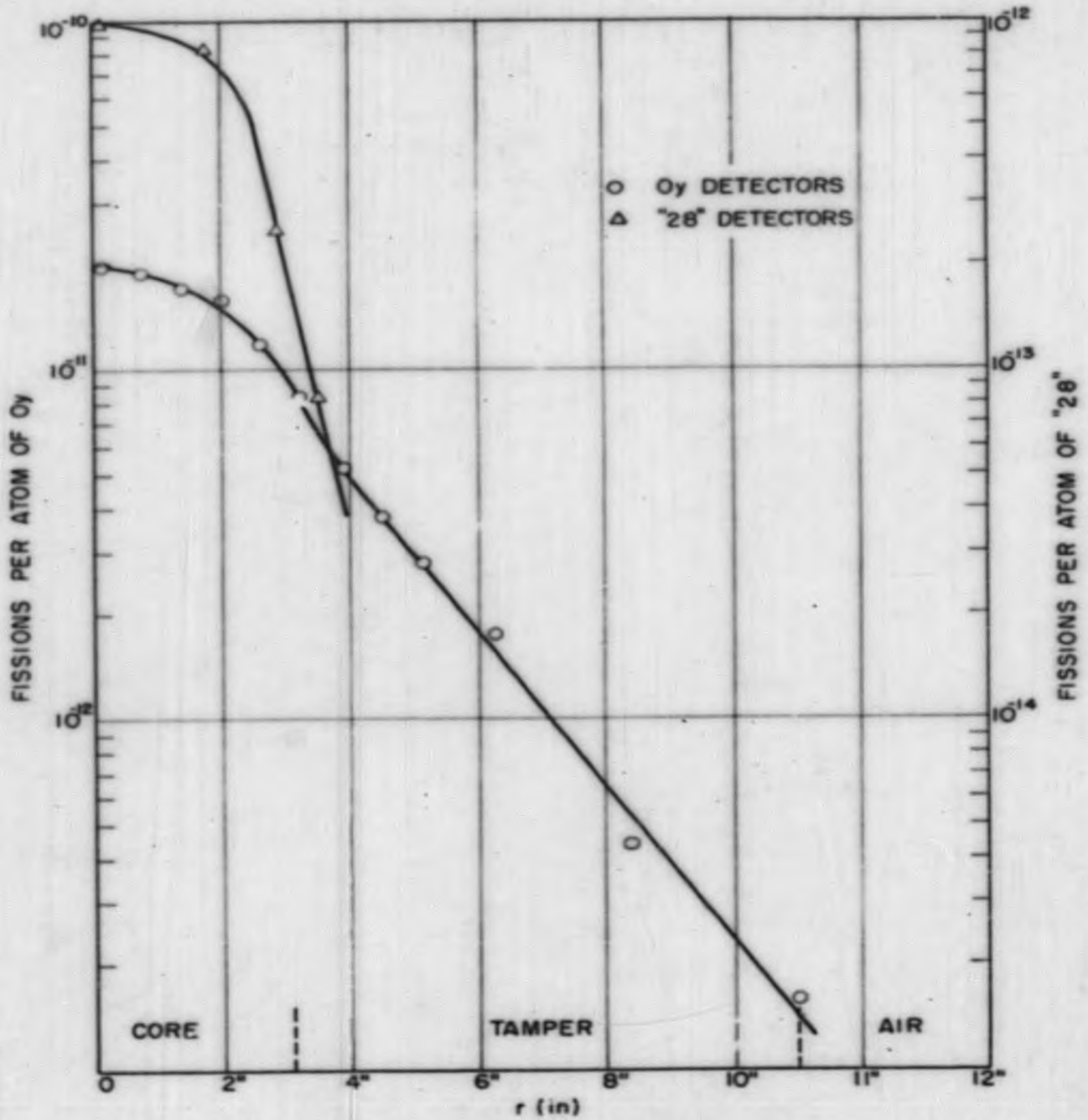


FIG III - 1 TOPSY - HYDRIDE IN Tu
-35-

SECRET

SECRET

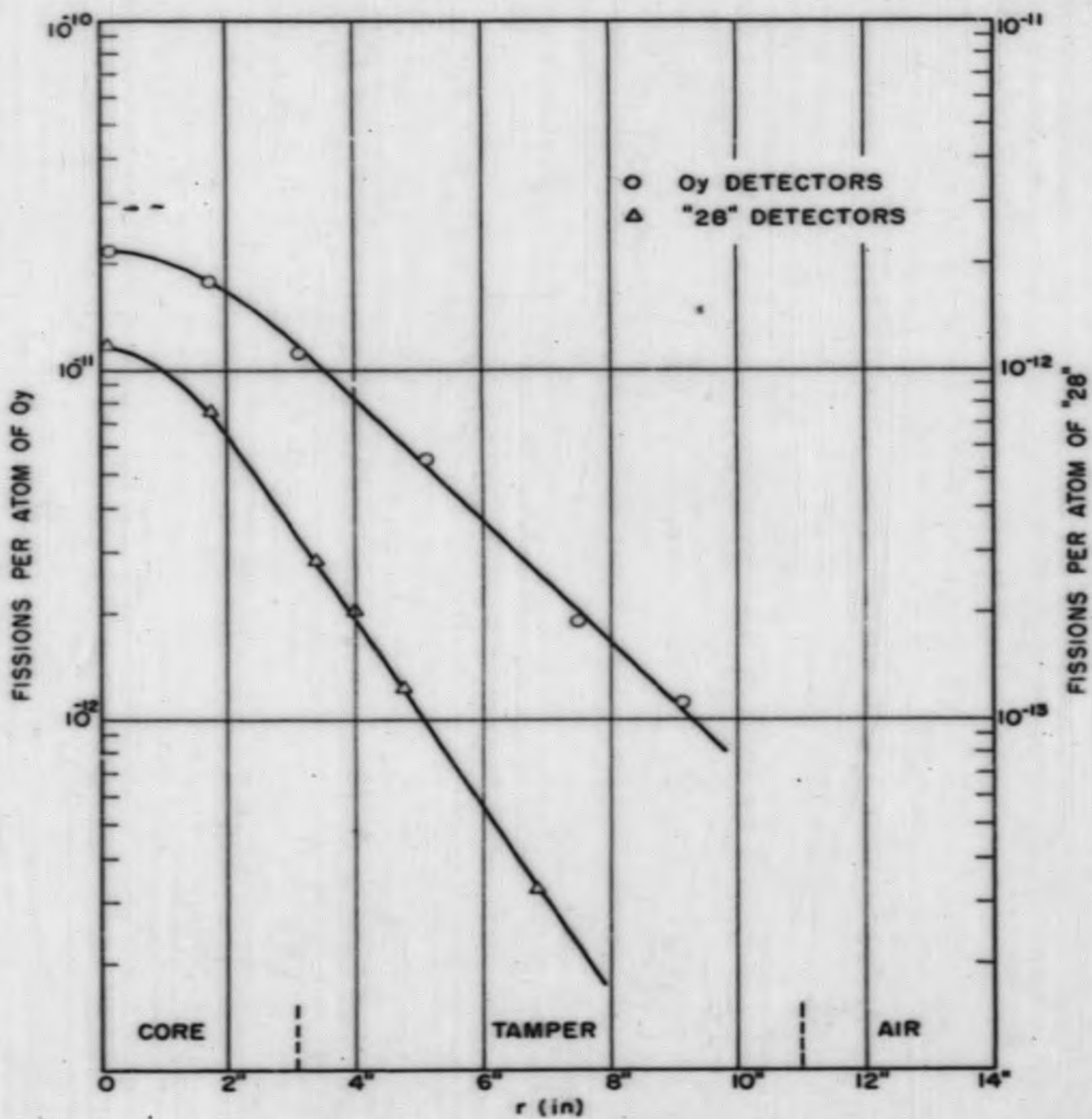


FIG. III - 2 TOPSY - HYDRIDE IN Ni

-36-

SECRET

SECRET

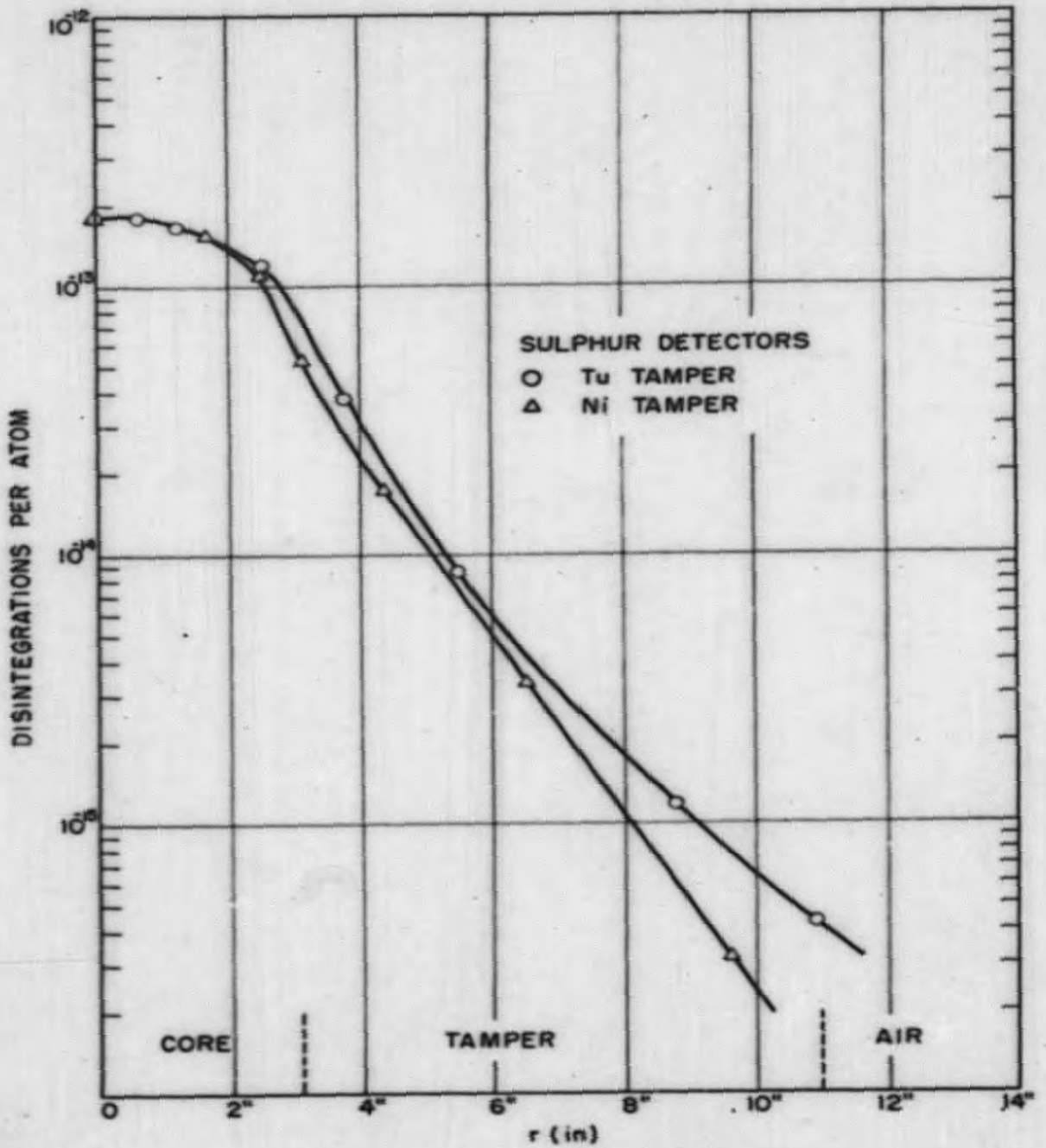


FIG. III - 3 TOPSY - HYDRIDE

-37-

SECRET

SECRET

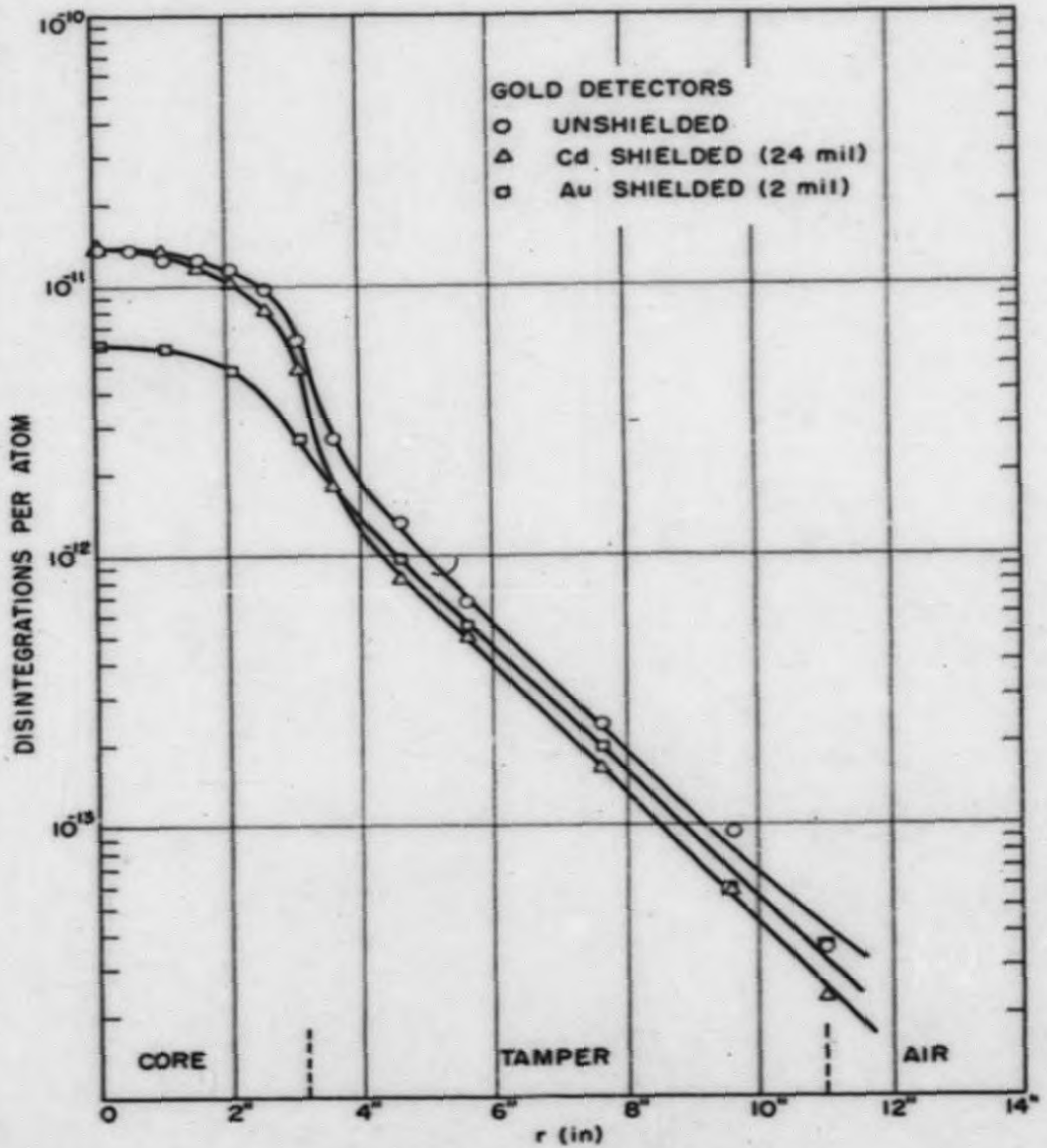


FIG. III - 4 TOPSY - HYDRIDE IN Tu

-38-

SECRET

SECRET

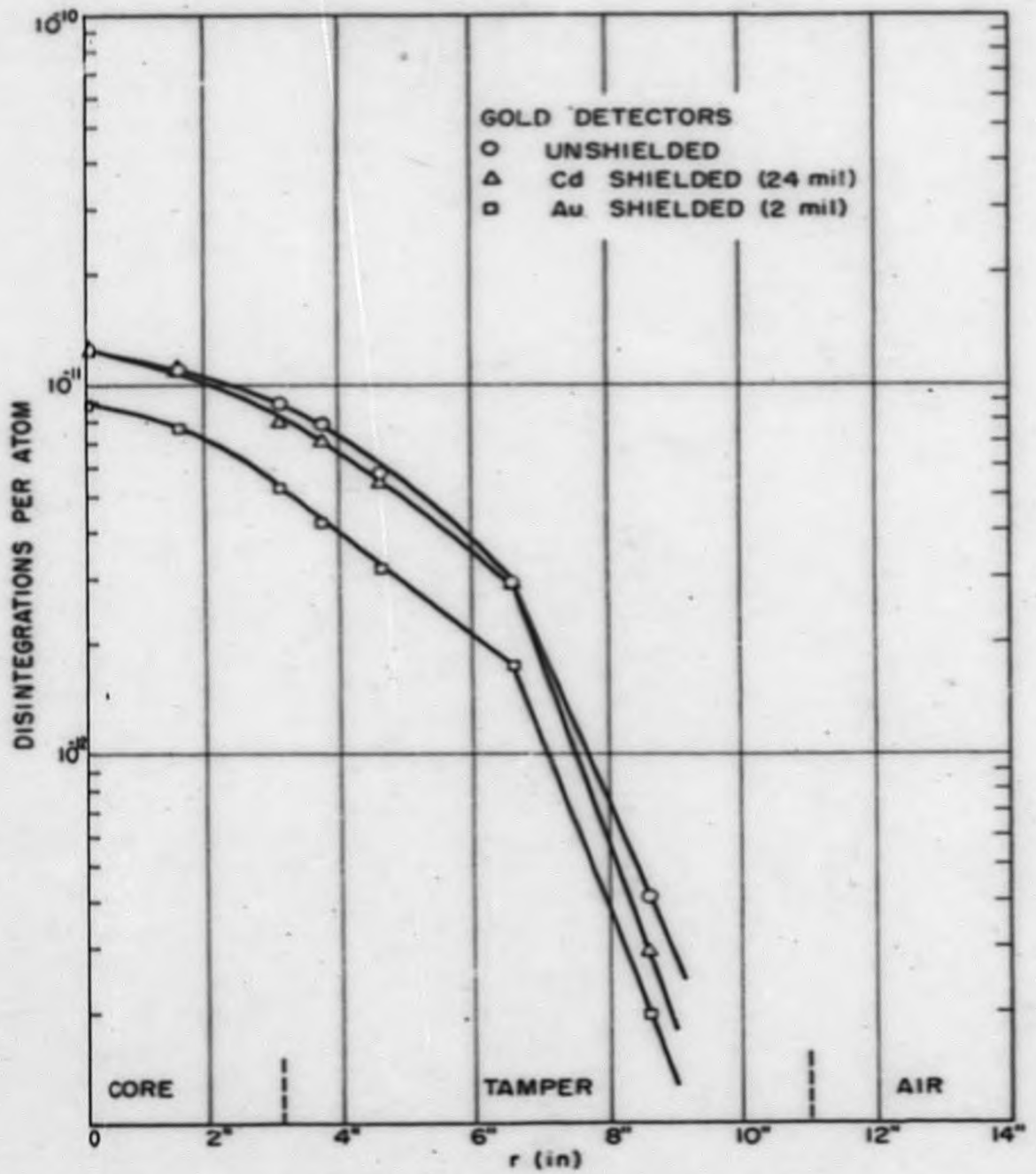


FIG. III - 5 TOPSY - HYDRIDE IN Ni

-39-

SECRET

SECRET

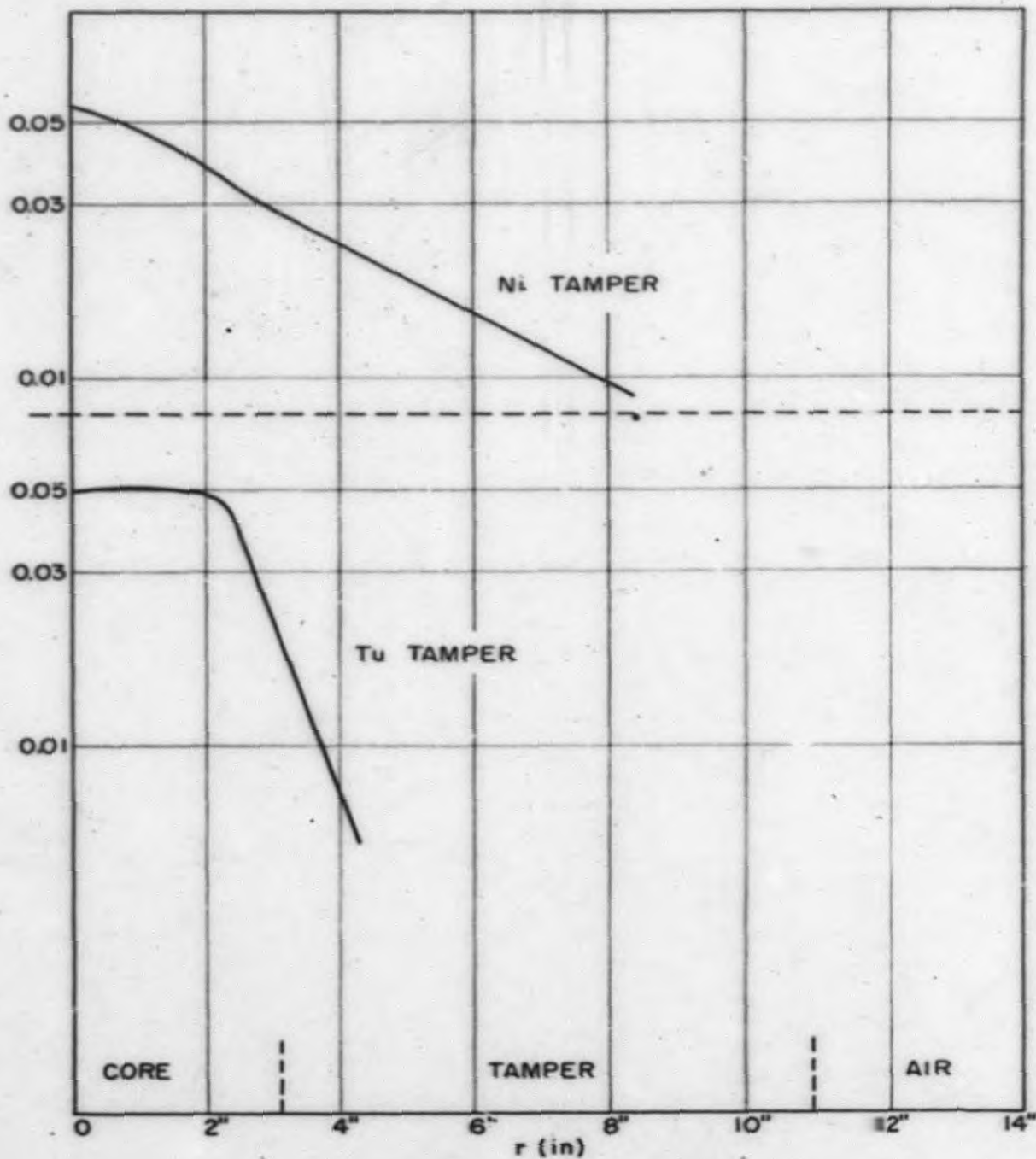


FIG. III-6 TOPSY-HYDRIDE
Ratio ^{28}Oy Fission Rates vs Radius

-40-
SECRET

S E C R E T

Two qualitative features of these curves are perhaps worth commenting upon. It is seen that the U^{238} fission rate falls off more sharply as a function of radius in the tuballoy tamper than it does in the nickel tamper. This behavior would seem to show that tuballoy more effectively shifts the neutron spectrum toward lower energies than does nickel. With this in mind, it might be expected that gold detectors should show activities which fall off more sharply in nickel than in tuballoy. Just the opposite of this is observed, however, in the first few inches outside of the core. Such a response is probably indicative of the fact that the low energy portion of the spectrum of neutrons emerging from the core has a longer capture mean free path in nickel than in tuballoy.

Aside from such qualitative considerations, however, the main value of these measurements lies in the opportunity offered for comparing observed detector responses with those predicted on the basis of Monte Carlo calculations, as a means of checking the assumed values of cross sections for elastic and inelastic scattering processes that go into such calculations.

S E C R E T

PART IV

EFFECTS OF FOREIGN MATERIALS IN HYDRIDE ASSEMBLIES

Method of Measurement

A survey of the effects on reactivity of various foreign materials in the hydride assemblies extended over a 5-month period. Most samples were elements or simple compounds (usually oxides) in the form of pressed or machined $\frac{1}{2}$ " cubes. Pressed specimens were prepared by the Powder Metallurgy Section of CMR-6. A few, in powder form, were in 0.5 gm Al containers, $\frac{1}{2}$ " diam. x $\frac{1}{2}$ " long. The materials came from a wide variety of sources and in most cases contaminants were not checked. The samples were introduced as near the hydride center as possible ($r \approx 0.8$ "), in the tamper adjoining the hydride ($r \approx 3.35$ " , interface at $r \approx 3.08$ ") and in some cases at intermediate positions.

Measurements were made in terms of control rod change required to restore the system to delayed critical when a sample was placed in a $\frac{1}{2}$ " cubic space (some early measurements on the hydride-Tu assembly were of reactivity changes when a hydride cube was replaced by a cube of the material investigated; as reduction of results to "air" reference magnified errors, most of these measurements were repeated under better conditions). By means of control rod calibration curves, Figs. IV-1 and IV-2, and sample masses, data were converted to reactivity change in cents per gm-atom or mole. The shapes of control rod calibration curves were obtained in terms of reciprocal multiplication and equivalent hydride mass as a function of control rod position. The cents scale was established by measurement of positive periods corresponding to shifts from delayed critical by known increments of control

SECRET

-43-

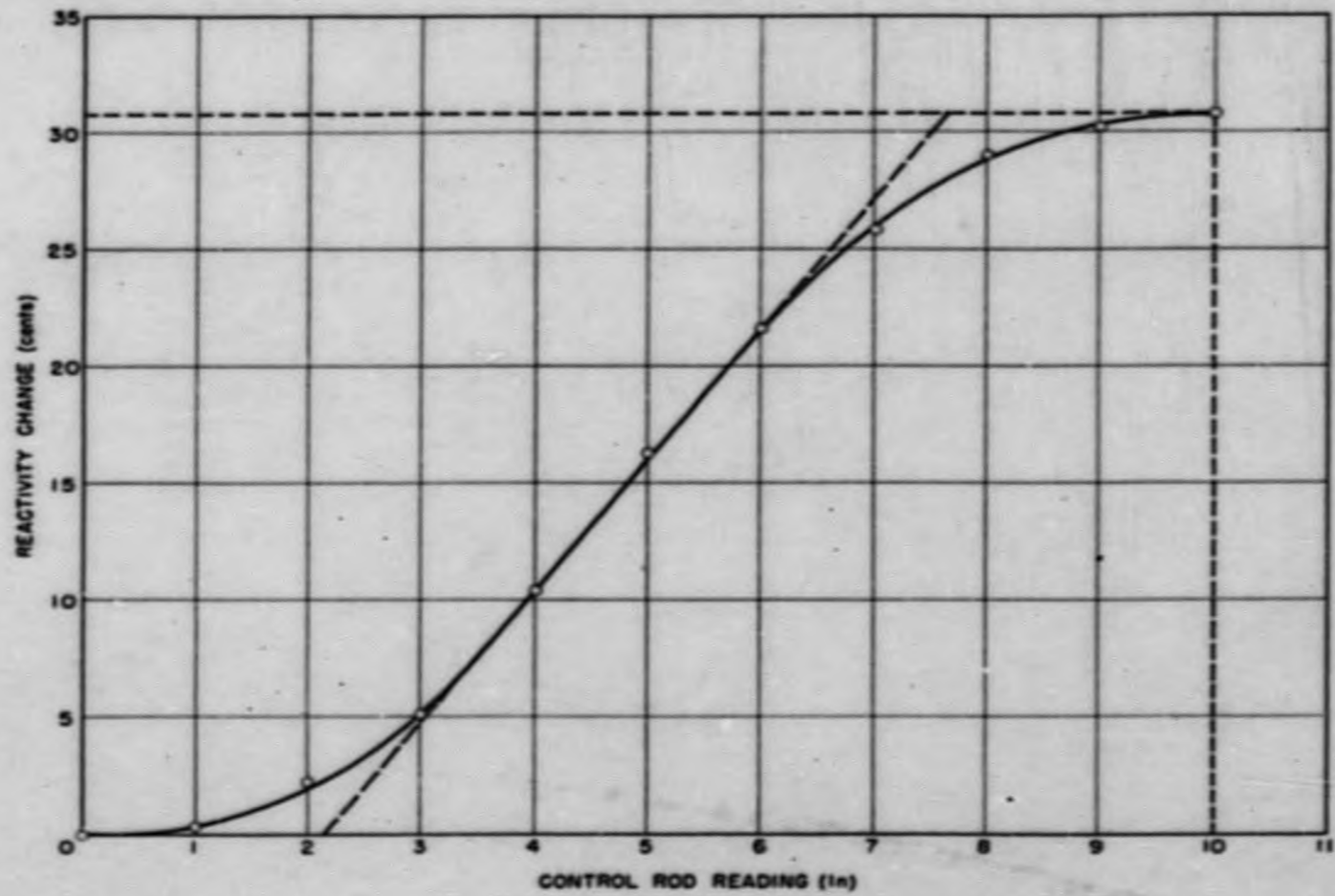
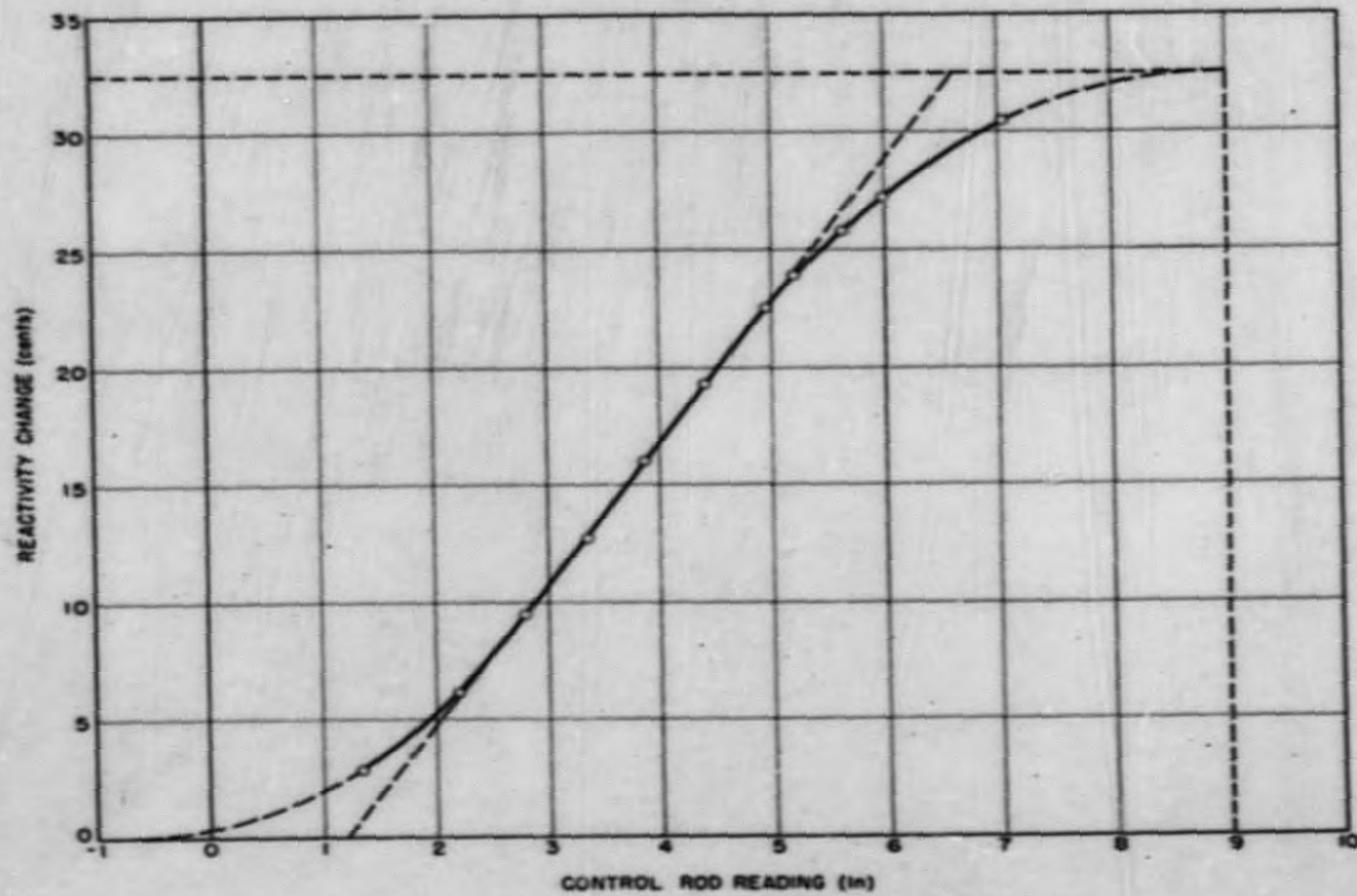


FIG. IX-1 CALIBRATION OF CONTROL ROD NO. 2
HYDRIDE - T_v ASSEMBLY

SECRET

SECRET

-44-



SECRET

FIG. III-2 CALIBRATION OF CONTROL ROD NO. 2
HYDRIDE - NI ASSEMBLY

S E C R E T

rod position. De Hoffmann's values⁽¹⁾ of delayed neutron periods and intensity ratios were used to convert to intervals from delayed critical in cents. As the cents scale is unimportant except to allow the comparison of results for different conditions, the details of this conversion are incidental.

Experimental Results

Results of measurements in the three radial positions most generally used are given in Table IV-1 for the Tu and for the Ni-tamped assemblies. The discussion of errors in the notes which follow this table leaves much to be desired, this is a consequence of the decision to devote necessarily limited efforts to a general survey instead of a careful study of a few materials. Several changes in technique in the course of this work presumably improved reliability of results but did not eliminate occasional inconsistencies.

The attempts to reconstruct reactivity changes for compounds and mixtures from values for the elements (values in parentheses for the last four items of Table IV-1), disagree considerably with data obtained directly. In the most important case, Oy-hydride, the average discrepancy is 10% for the Tu tamped assembly and 5% for the Ni tamper. The most careful check on additivity of results was a comparison of measurements on a Pu cube with measurements on the difference between two Pu cubes which differ in weight by 0.92 gm. Based on the 0.92 gm difference, the Pu value is 226 cents/gm-atom (0.8" position, Ni tamper). This compares with $243\frac{1}{2}$ cents/gm-atom as an average of several values based on 28-29 gm cubes. The difference, 7%, corresponds to an effective error of 0.06 gm Pu (in 0.92 gm) whereas the greatest sensitivity indicated by response to control rod settings is about

(1) Delayed Neutrons from U²³⁵ after Short Irradiation, F. de Hoffmann, B. T. Feld and P. R. Stein, *Phys. Rev.* 74, p. 1330 (11/15/48).

SECRET

TABLE IV-1

EFFECTS OF FOREIGN MATERIALS IN HYDRIDE ASSEMBLIES

reactivity change in cents per gm-atom or mole

Z	Material	0.8"		2.4"		3.35"	
		Tu Temper	H1 Temper	Tu Temper	H1 Temper	Tu Temper	H1 Temper
1	H ⁽¹⁾	38.5	44	22.5	26.5	5	9
4	Be	<u>10</u>	12	8.5	12.5	<u>5</u>	6.5
5	B	-59.5	-68.5	-30.5	-34.5	<u>-5</u>	-12
6	C	4.5	4.5	6.5	8.5	<u>5</u>	6
7	? H ⁽²⁾	<u>16</u>				<u>7.5</u>	
8	O ⁽³⁾	5	4	<u>5</u>		<u>5</u>	5.5
12	Mg	9.5	11.5	12	13.5	<u>5.5</u>	8
13	Al	2.5	4.5	7	8.5	<u>3.5</u>	5
14	Si	3.5	3			4.5	3.5
15	? P	<u>12</u>				<u>6</u>	
16	S	-1	-0.5			1	1.5
21	Se ⁽⁴⁾⁽⁵⁾	<u>9.5</u>					
22	Ti	<u>3.5</u>	7			<u>8</u>	7
23	V	3.5	4.5	10	10.5	<u>10.5</u>	8.5
24	Cr	<u>5</u>				<u>5.5</u>	
25	Mn	-2	-2	5.5	10	<u>8.5</u>	6
26	Fe	2.5	4.5			6	5.5
27	Co	-9.5	-8.5	1	3.5	<u>5</u>	4
28	Ni	-0.5	1	7	8	<u>7.5</u>	6
29	Cu	2	3.5			5.5	6.5
30	Zn	4	3.5			6.5	6.5
32	Ge ⁽⁵⁾	3		3			
33	As	-13	-9.5			5	4

SECRET

TABLE IV-1

		0.8 ^m		2.4 ^m		3.75 ^m	
		<u>Tu</u>	<u>Hi</u>	<u>Tu</u>	<u>Hi</u>	<u>Tu</u>	<u>Hi</u>
39	<u>r</u> (4)(5)	<u>-1</u>					
40	<u>Ir</u> (4)(5)	<u>14</u>					
41	Cb	-5	-3.5			6.5	5.5
42	Mo	-2.5	-0.5			7.5	9
45	Rh	-39.5				<u>1</u>	
46	Pd	-20	-17.5			4	2
47	Ag	-19.5	-51			-0.5	-6
48	Cd	-19	-17	-3.5	1.1	<u>3.5</u>	3
49	In	-53	-56.5			-1.5	-9
50	Sn	<u>-0.5</u>	2			5.5	7.5
51	Sb	-31.5	-32			-0.5	-3
52	Te	-5	-4.5			4	2.5
53	I	-53				<u>1</u>	
57	? <u>La</u> (5)	<u>70</u>		<u>53</u>		<u>28</u>	
58	<u>Ce</u> (4)	<u>33</u>				<u>15.5</u>	
60	<u>Nd</u> (4)(5)	<u>3</u>					
62	? <u>Sm</u> (5)	-172		-60		<u>10</u>	
64	<u>Gd</u> (4)(5)	<u>-182</u>				<u>-1</u>	
68	? <u>Er</u> (4)(5)	<u>-58.5</u>					
73	Ta	-69	-69	-29.5	-28	<u>-2</u>	-9
74	W	-22	-22.5	-4.5	-4.5	<u>5.5</u>	3.5
76	<u>Os</u> (5)	<u>-53</u>		-19		<u>7.5</u>	
78	Pt	-21.5	-20.5			5.5	3.5
79	Au	-11	-10	-11.5	-9.5	<u>2</u>	-1
81	Tl	-1	4.5			8	6.5
82	Pb	4	7			10.5	12

TABLE IV-1

		0.8"		2.4"		3.35"	
		Tu	Ni	Tu	Ni	Tu	Ni
83	Bi	7	8	16	18.5	9.5	11.5
90	Th ⁽⁶⁾	<u>19</u>	23	<u>23.5</u>	35.5	<u>6</u>	19
92	U	12	17.5	<u>12.5</u>	19.5	<u>10</u>	10
92	Oy	<u>119</u>	134.5	77.5	82	<u>50.5</u>	43
94	Pu	<u>220</u>	243	133	141.5	<u>81.5</u>	69
	WC	-25(-17.5)	-22(-18)			9.5(10.5)	6.5(9.5)
	Oy _{2.97} C _{1.11} O _{0.25} ⁽⁵⁾	215(210)	254(272)	133(153)	166(171)	76(73)	
	UH _{3.23} C _{.89} O _{.18} ⁽⁵⁾	109(141)		72.5(92)			
	C ₅ H ₈ O ₂ ⁽⁵⁾	328(340)		182(222)		74(75)	

- (1) From measurements on polythene and C.
- (2) From measurements on TiN and Ti.
- (3) From measurements on Al₂O₃ and Al.
- (4) From measurements on the oxide.
- (5) Samples small, so errors per ga-atom relatively large.
- (6) Results not reproducible, evidence of systematic change (low density pressed powder sample).

Values in parentheses computed from results for component elements; several steps involved so errors magnified.

Operation more stable for measurements giving underlined values than for others.

Errors: A number of underlined values were from repetitions of earliest measurements. For 21 normal samples, differences ranged from 0.0 to 0.8 unit, corresponding to a probable error of ± 0.3 unit (in relative values for a given tamper). In addition, there were 4 wild cases with differences of 1.4 to 2.9 units. Absolute values (for comparison between Tu and Ni tampers) have an added uncertainty which should be within $\pm 5\%$. Systematic differences (between Tu and Ni tampers) may suggest a larger calibration error.

S E C R E T

0.0) gm Pu.

After completion of hydride measurements, it became apparent that identification of rare earth samples by label is extremely risky. Spectroscopic analysis by CMR-1 of the Sm (metal) used for these investigations gave 10% Sm, Major Y content, 10-20% Dy and possibly 10% Gd. Similarly, Er_2O_3 ("pure") gave strongest indication of Y, with about 10% Dy and less than 1% Er. As the effect of Y in the hydride assembly was essentially neutral, the large negative value for "Sm" probably consists of contributions by Sm, Gd and Dy (each known to have large total cross section for low energy neutrons) and for "Er" the effective element must be Dy.

Doubt also has been cast on the compositions of La, P and TiN samples. The La sample again gave a large positive effect in an O_y metal assembly, which was not confirmed with a vacuum cast piece of pure La loaned by CMR-5. If the "La" specimen were for example, LaH_2 , the H content could account for the reactivity changes observed within a radius of 2.5" (see Fig. IV-6). Attempts to obtain quantitative information about "small quantities of paraffin" used to bond P and TiN powder in the specimens used led to the suspicion that H may have contributed appreciably to the effects attributed to P and N.

Variation with Z

Reactivity changes per gm-atom for the nearly central position in the Tu taped assembly are given as a function of Z in Fig. IV-3. The general features of downward trend from $Z=1$ to $Z=50$ and grouping of even Z elements above odd Z agree (though not in magnitude) with observations on other

SECRET

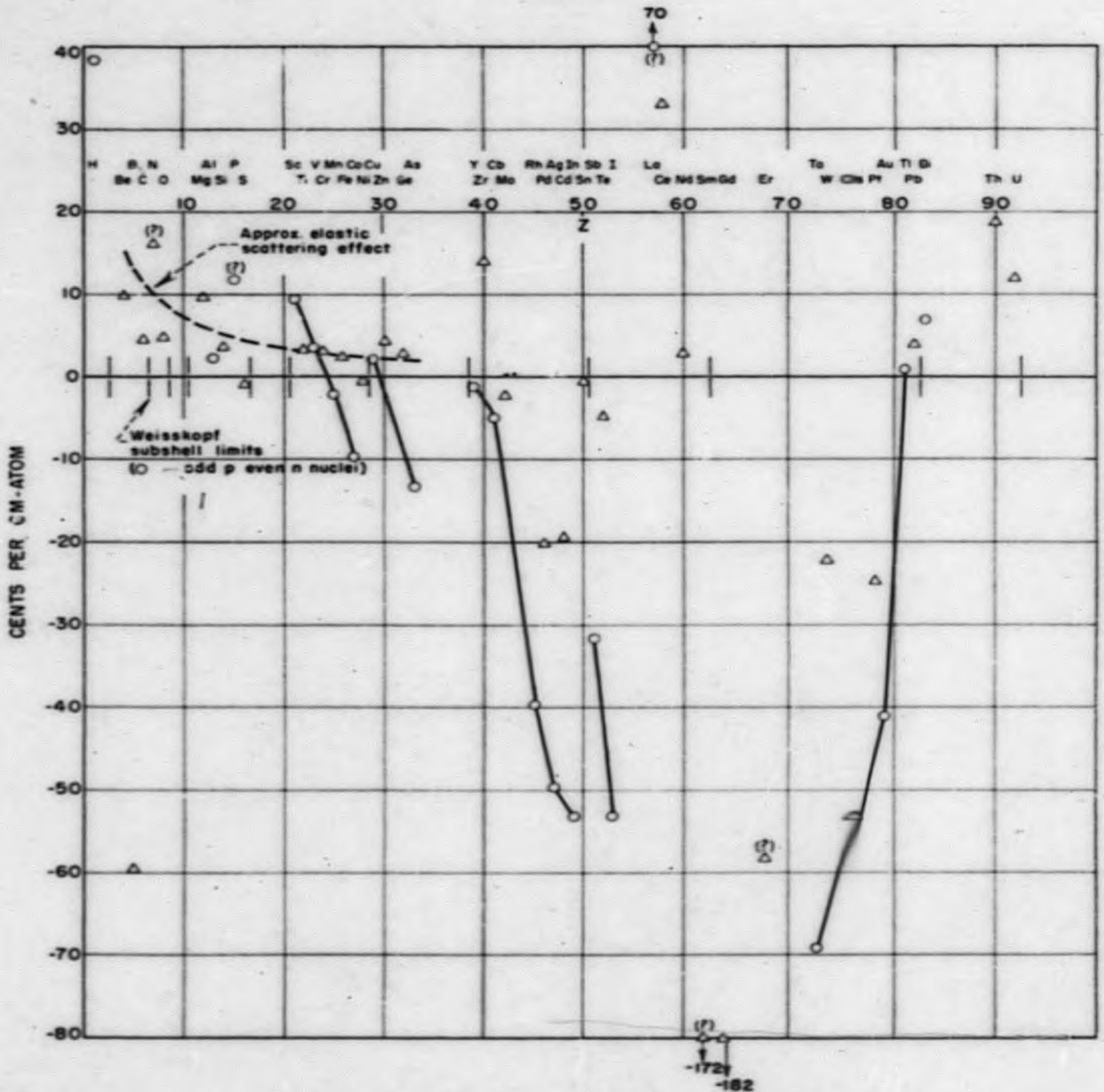


FIG. III-3 REACTIVITY CHANGE PER GM-ATOM vs. Z CENTER OF HYDRIDE-Tu ASSEMBLY

S E C R E T

assemblies. (2) (3) The rare earth region appears to be one of extremes, and above $Z=73$, the trend is upward.

Positive effects of non fissionable materials near the core center, of course, must be attributed to neutron energy degradation by scattering. As inelastic scattering for $Z \sim 30$ and for the relatively low energy neutrons of the hydride is believed to be negligible, (4) it is necessary to turn to elastic scattering effects to account for positive energy contribution by relatively light elements. The order of magnitude of the reactivity contribution per gm-atom, R_A in cents/gm-atom, by an elastic scatterer (atom weight A and scattering cross section $(\bar{\sigma}_s)_A$) may be obtained as follows.

$$\frac{R_A}{R_{25}} = \frac{(\bar{\sigma}_s)_A (M_S - 1)_A}{(\bar{\sigma}_f)_{25} (\nu - 1 - \alpha)_{25}}, \text{ where } M_S \text{ is the effective neutron}$$

multiplication per scattering. The neutron energy loss by scattering, the average being given by

$$\Delta E/E = - \frac{2}{A + 1},$$

leads to an increase in fission probability, P_f , such that

$$(M_S - 1) = \frac{\Delta P_f}{P_f} \approx \frac{\Delta (\sigma_f)_{25}}{(\sigma_f)_{25}} = \left(\frac{\partial (\sigma_f)_{25}}{\partial E} \frac{E}{(\sigma_f)_{25}} \right) \frac{\Delta E}{E}.$$

Actually $\Delta (\sigma_f)_{25} / (\sigma_f)_{25}$ is a slight overestimate of $\Delta P_f / P_f$

because, for neutrons near the core center $P_f \approx \frac{1}{2}$ and the two expressions agree for $P_f \ll 1$.

(2) Average Effective Cross Sections for the Fast Plutonium Reactor Spectrum, Hall and Hall, LAMS-734 (7/9/48).

(3) KAPL Progress Report No. 39, Section II, Reactor Physics, KAPL-265 (10/1-31/49).

(4) Cross Sections for Fast Neutrons, Part II, H. H. Barschall, et al, Phys. Rev. 72, p 881 (11/15/47).

S E C R E T

Now, from $(\sigma_f)_{25}$ vs neutron energy (e.g. from LA-140):

$$\frac{d(\sigma_f)_{25}}{dE} \frac{E}{(\sigma_f)_{25}} \approx -0.4, \quad 50 \text{ ev} < E < 500 \text{ Kev};$$

$$\text{so } (M_S - 1)_A \approx \frac{0.8}{A + 1},$$

$$R_A \approx \frac{0.8}{A + 1} \frac{(\overline{\sigma_S})_A}{(\overline{\sigma_f})_{25} (\overline{v-1-w})_{25}} R_{25}.$$

Taking $R_{25} = 133$ cents/gm-atom,

$$(\overline{\sigma_f})_{25} = 3 \text{ b},$$

$$(\overline{v-1-w})_{25} = 1.4,$$

and $(\overline{\sigma_S})_A = 6 \text{ b}$, an average for elements tested in the range $4 \leq Z \leq 32$, we have

$$R_A \approx \frac{150}{A + 1} \text{ cents/gm-atom.}$$

This relation, shown for low Z by the dotted line in Fig. IV-3, is of the correct order of magnitude to account for the observed positive effects.

Points for odd proton, even neutron nuclei are encircled in Fig. IV-3. These generally form groups within which trends are preserved. Values of Z at which nuclear subshells are completed, according to Weiskopf's modification of Mayer's scheme ⁽⁵⁾ (Z 's shown by dashes), fall into gaps between the indicated groups. It should be mentioned that agreement is poorer for

⁽⁵⁾ Symposium on Nuclear Shell Structure, American Physical Society Meeting at New York City (2/4/50)

S E C R E T

other nuclear level schemes such as that of Feenberg and Hammack⁽⁶⁾. The only irregularities involve P and La, samples of which are questionable.

Variation With Radius

Figs. IV-4, IV-5, and IV-6 indicate for some of the more interesting materials, reactivity changes per gm-atom or mole as a function of radial position within the assembly. As mentioned previously, the reactivity changes are for a configuration which is unchanged except for addition of the material of interest.

In Fig. IV-4 are grouped curves typical of pronounced neutron absorbers. B, Au and Cd, of course, are known to have large absorption cross section for low energy neutrons. Ta, similarly effective, may be of interest because of potentially good mechanical properties. Mn, in the Tu tamped assembly, is included as typical of a transition case in which a good tamper (for a static assembly) has measurable absorption near the center of the core. A striking difference between curves for Ni tamped and for Tu tamped assemblies is that the latter rise more abruptly in the outer part of the hydride core. This and a similar difference between ratios of 25 to 28 fission catcher activities for the two assemblies (Fig. III-6) are consistent with greater degradation of energy of neutrons returning to the core from the Tu tamper than from the Ni tamper.

Fig. IV-5 gives reactivity change results for elements of interest as tampers. The general difference in shape of curves for Tu and for Ni tampers,

(6) Nuclear Shell Structure; Feenberg and Hammack; Phys. Rev. 75, p 1877 (6/15/49)

SECRET

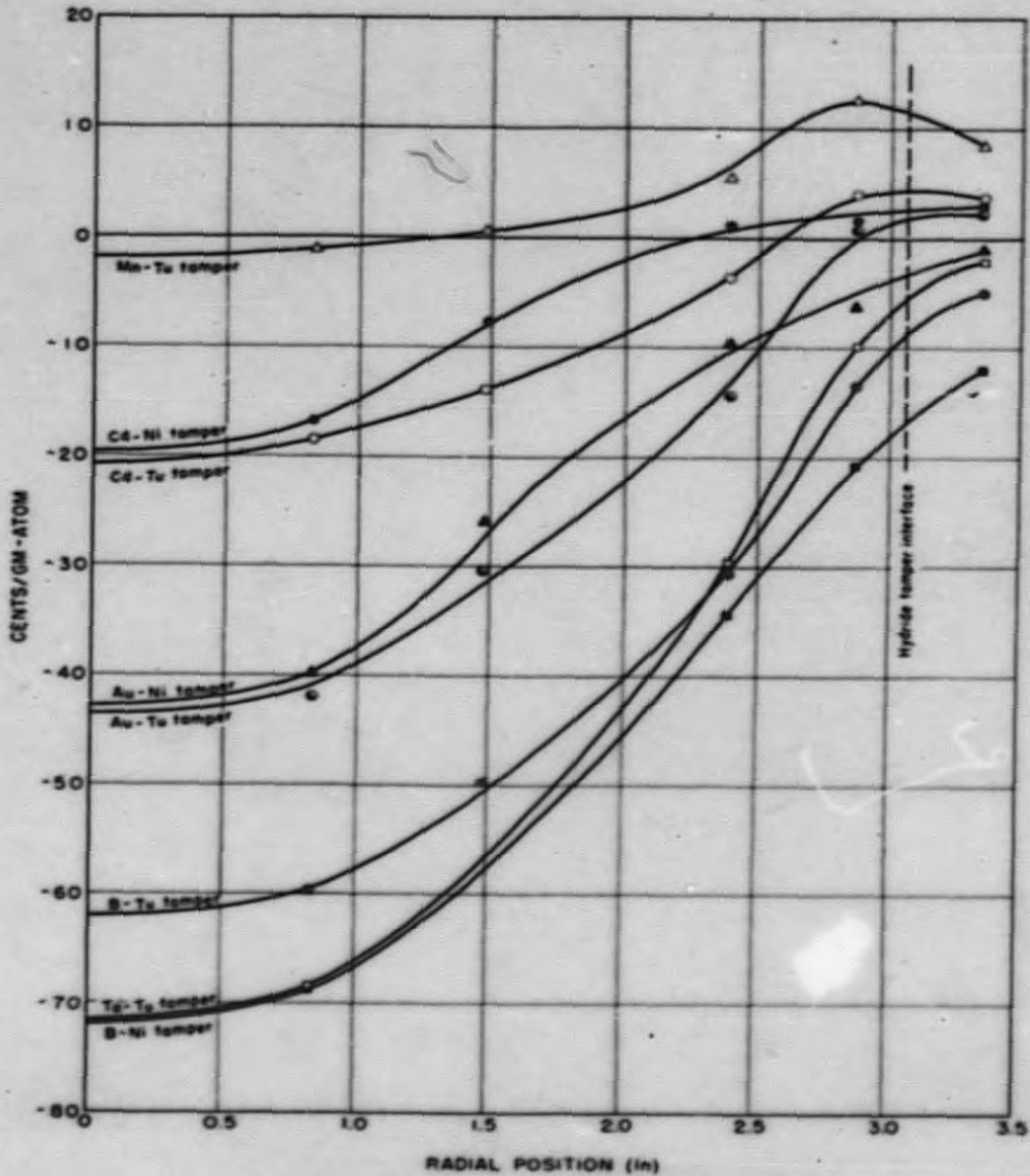


FIG. IX-4 REACTIVITY CONTRIBUTIONS BY MATERIALS
ADDED TO HYDRIDE ASSEMBLIES

NEUTRON ABSORBERS
-54-

SECRET

SECRET

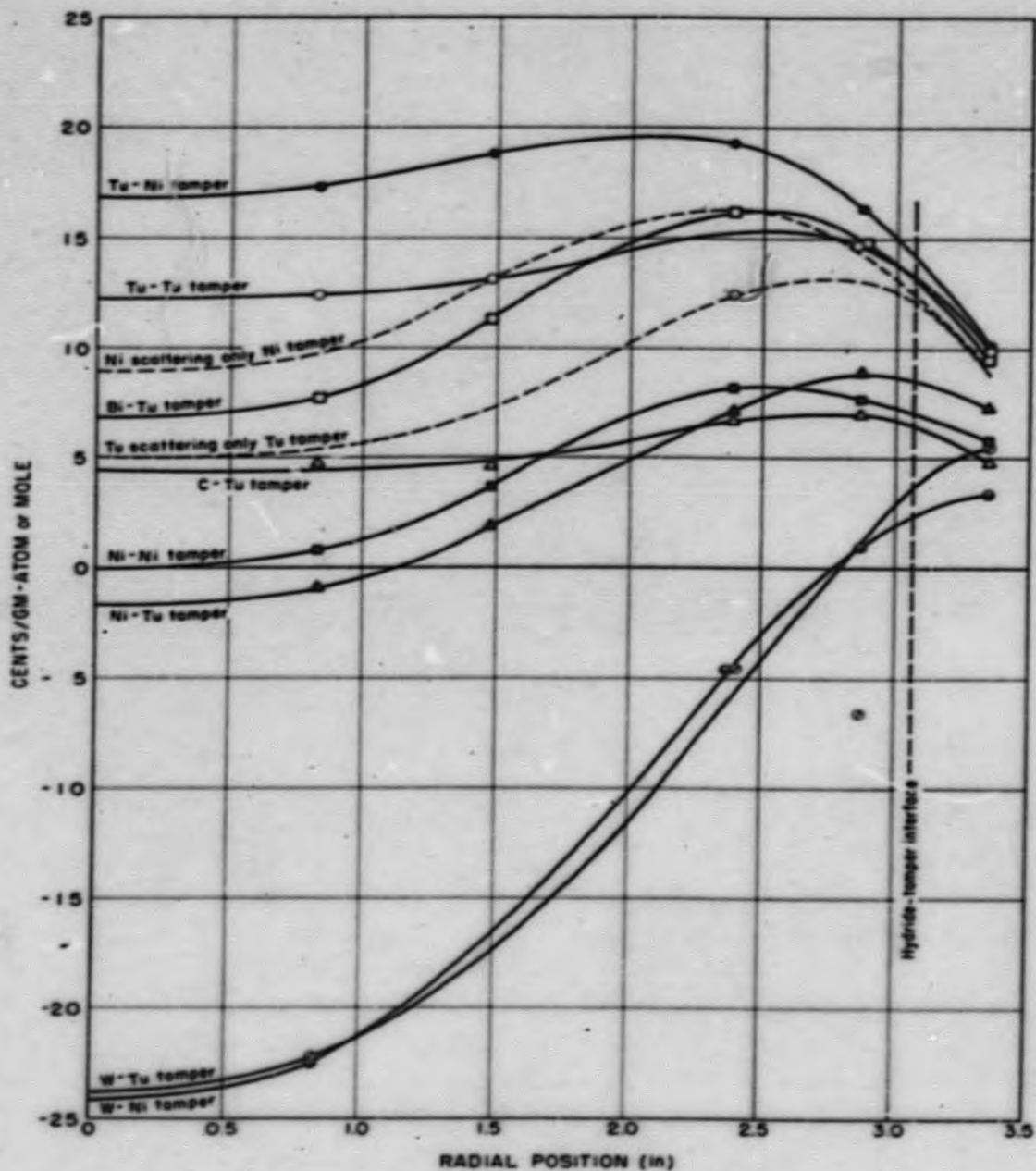


FIG. IX-5 REACTIVITY CONTRIBUTIONS BY MATERIALS
ADDED TO HYDRIDE ASSEMBLIES

ELEMENTS OF INTEREST IN TAMPERS

-55-

SECRET

SECRET

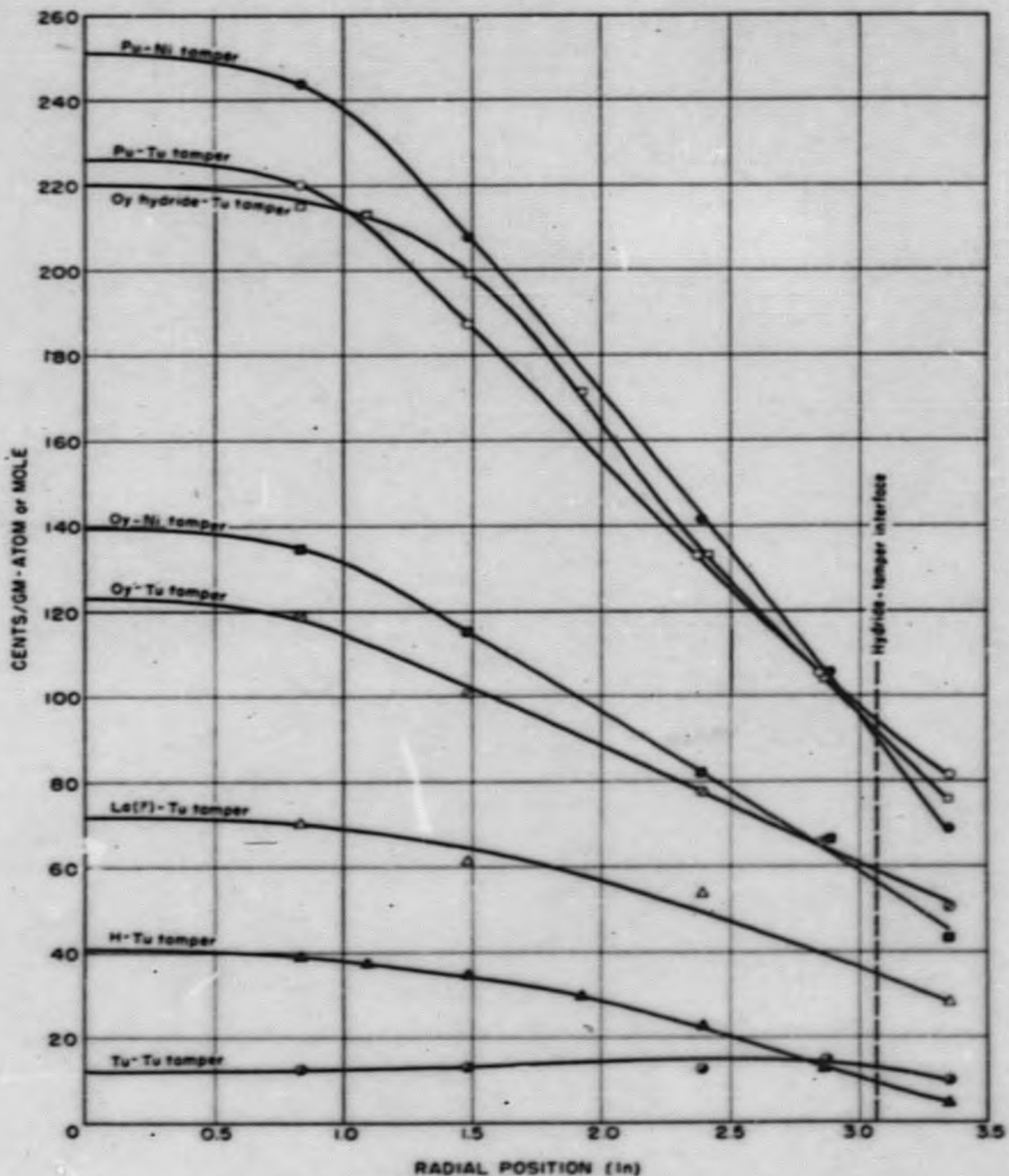


FIG IX-6 REACTIVITY CONTRIBUTIONS BY MATERIALS
ADDED TO HYDRIDE ASSEMBLIES
FISSIONABLE MATERIALS, ETC.

SECRET

S E C R E T

which was noted for the absorbers, seems to be maintained. The W curves, typical of absorbers, appear to be out of place in the tamper family. Scattering and absorption contributions by Tu, i.e., with fission effects subtracted, are indicated by the dotted curve for the Ni tamper and the dashed curve for Tu tamper. Fission effects of 28 were estimated by applying 28 to 25 fission catcher activity ratios (Fig. III-6) to 25 reactivity changes resulting from fission (from Fig. IV-6).

Although reactivity changes per gm-atom are greater for Tu than Ni at the position outside the hydride (3.35" radius), per unit volume, Ni is 1.4 times as effective as Tu for the Tu tamper and 1.1 times as effective for the Ni tamper. This consideration led to the critical mass measurements on Ni lined Tu tampers, which were described in Part I.

Reactivity change-radius curves for materials which show a large positive contribution near the core center are given in Fig. IV-6. A Tu curve is repeated to emphasize the scale. Degradation of neutron energy by single-step elastic scattering can account for the large central effect of H.

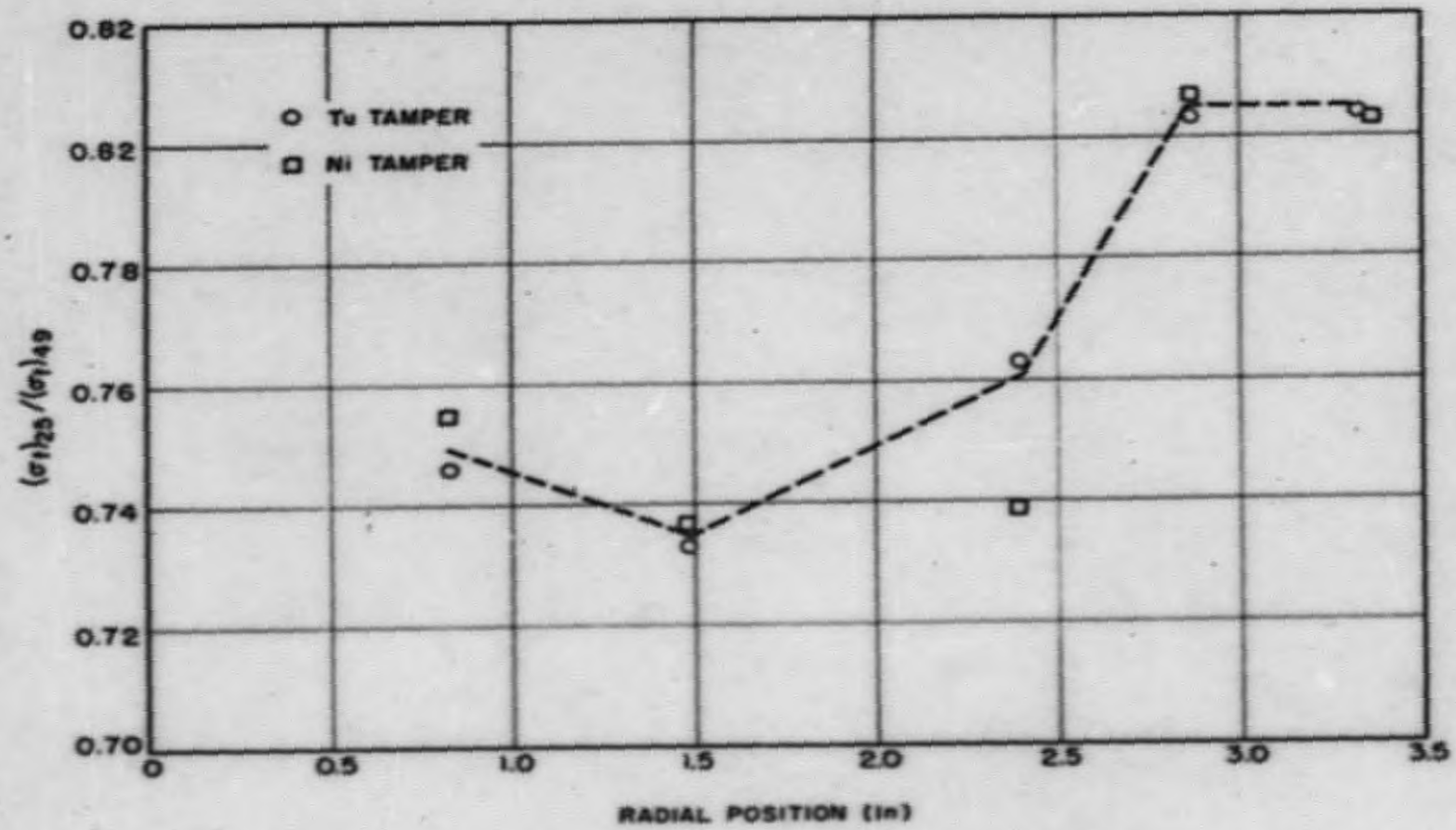
From the Oy and Pu data, the ratio of effective fission cross sections, $\overline{\sigma}_f(25) / \overline{\sigma}_f(49)$, may be obtained. The Oy curve is corrected for 28 contribution and both 25 and 49 are corrected for scattering on the assumption that it is the same as for Tu (for the latter correction, Tu data in turn are corrected for fission). If $\beta-1-\alpha = 1.52$ for 25 and 2.02 for 49⁽⁷⁾ (appreciable α reduces these values), the fission cross section ratios of Fig. IV-7 are obtained. In cases where the principal contributors are

(7)

Neutron Multiplication in Subcritical Spheres, A. Hanson and H. L. Anderson, LA-1033 (12/19/47).

~~SECRET~~

-58-



~~SECRET~~

FIG. IV-7 RATIO OF FISSION CROSS SECTIONS OF 25 AND 49 IN HYDRIDE ASSEMBLIES

neutrons with energies appreciably above thermal, where $\sigma_f(25)/\sigma_f(49)$ changes monotonically (LA-140), each cross section ratio may be interpreted as an "effective" neutron energy. Although this may apply to an OY metal assembly, for hydride, neutrons of low energy probably are sufficiently important to complicate the interpretation. Considering that

$$\sigma_f(25) / \sigma_f(49) > 1 \text{ for } \sim 50 \text{ eV} < E_n < 100 \text{ Kev,}$$

and

$$\sigma_f(25) / \sigma_f(49) < 1 \text{ for } E_n < \sim 50 \text{ eV and } E_n > 100 \text{ Kev,}$$

the increase in $\sigma_f(25) / \sigma_f(49)$ with radial position in the hydride may represent depletion of either low energy or high energy end of the neutron spectrum, or of both ends. The decrease with radius of ratio of fission rates of 26 and 25 (Part III), points to a high energy influence, but appreciable self absorption of gold, for example, indicates additional low energy contribution to the observed change in cross section ratio.

Critical Mass of OY H₃ at $\rho = 7.0$

Material replacement data provide a means of computing the effect on critical mass of small changes in core composition and density. As an illustration, the critical mass in Tu of OYH₃ at a density of 7.0 gm/cm³ will be determined.

Reactivity changes per mole at various radii for OYH_{2.97}^{C1.11}_{O.25} (the estimated composition of the hydride sample inserted for measurement) may be converted by means of data for H, C and O to corresponding values for OYH_{2.93}^{C1.06}_{O.26} (the mean composition of the hydride core) and for OYH₃. The reactivity change per mole of OYH_{2.93}^{C1.06}_{O.26} at density ρ_0 and molecular weight M_0 is $R_0(r)$, the reactivity change per unit volume is $R_0\rho_0/M_0$. Similarly, for OYH₃ of density ρ and molecular weight M and

~~SECRET~~

reactivity change per mole $R(r)$, the contribution per unit volume is $R\rho/M$. Then the reactivity decrease which results when $\text{OyH}_{2.93}\text{C}_{1.08}\text{O}_{0.26}$ (density ρ_0) is replaced by OyH_3 (density ρ) throughout the original core of radius r_0 is

$$\Delta R = 4\pi \int_0^{r_0} \left(R_0 \frac{\rho_0}{M_0} - R \frac{\rho}{M} \right) r^2 dr.$$

To maintain the reactivity level of the original configuration, the core volume must be increased by a volume ΔV_c such that the reactivity increase in replacing Tu (ρ_u, M_u, \bar{R}_u averaged for ΔV_c) by OyH_3 (ρ, M, \bar{R} averaged for ΔV_c) equals ΔR . This reactivity contribution may be expressed

$$\Delta R = \Delta V_c \left(\bar{R} \frac{\rho}{M} - \bar{R}_u \frac{\rho_u}{M_u} \right).$$

Fig. IV-8 gives $4\pi \left(R_0 \frac{\rho_0}{M_0} - R \frac{\rho}{M} \right) r^2$ as a function of r in cm, where

$$\rho_0 = 7.35 \text{ gm/cm}^3, M_0 = 255,$$

$$\rho = 7.00 \text{ gm/cm}^3, M = 238.$$

Graphical integration to $r_0 = 7.8$ cm gives $\Delta R = 222$ cents. Then the change in critical volume,

$$\Delta V_c = 222 / \left(\bar{R} \frac{\rho}{M} - \bar{R}_u \frac{\rho_u}{M_u} \right),$$

$$\rho_u = 19.0 \text{ gm/cm}^3, M_u = 238,$$

may be evaluated (by successive approximation, $\bar{R} = 82$ cents/mole and $\bar{R}_u = 12.6$ cents/gm-atom) as

$$\Delta V_c = 158 \text{ cm}^3.$$

Thus, for OyH_3 ($\rho = 7.0$) in a thick Tu temper, the critical volume would be 2160 cm^3 , the critical mass 15.1 kg and the critical radius 8.02 cm ($3.15''$).

Deduced Relation Between Critical Mass and Density

From the reactivity changes per mole of hydride and Tu, a relation between

~~SECRET~~

~~SECRET~~

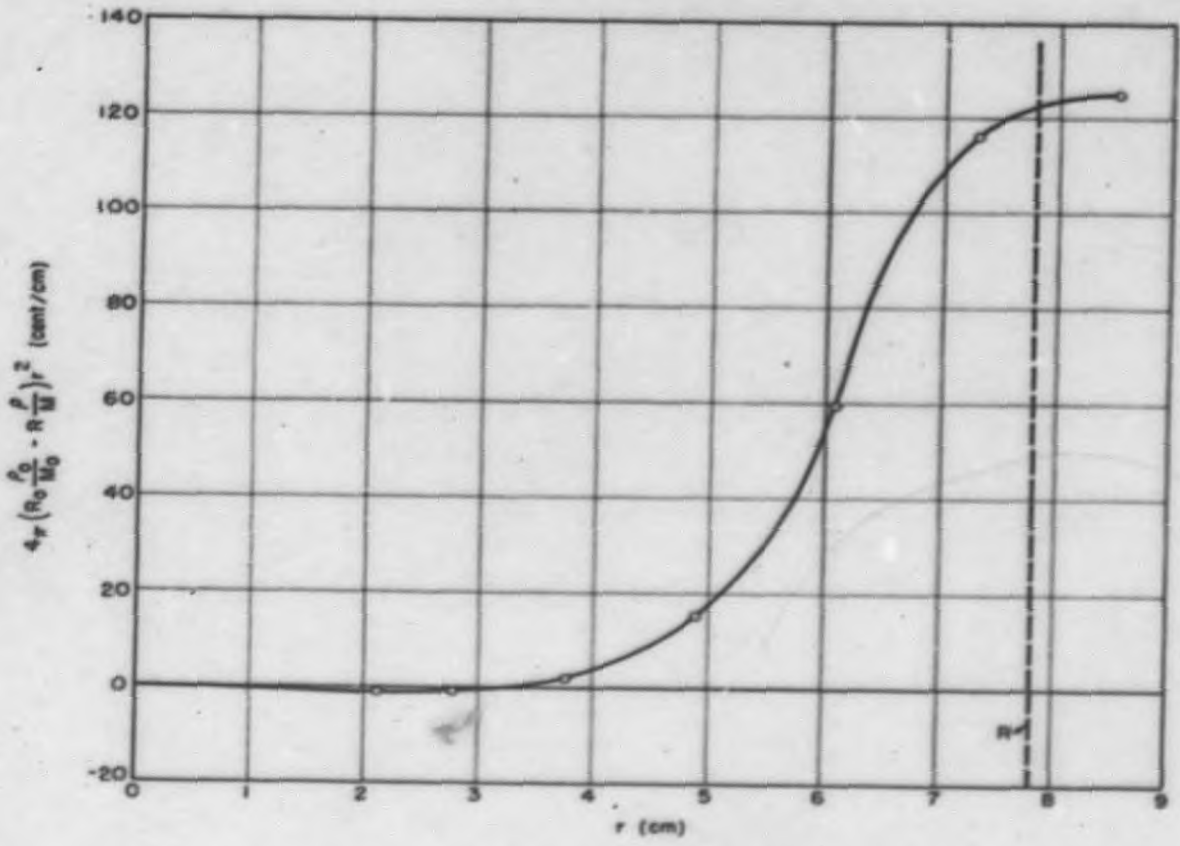


FIG. IX-8 CRITICAL MASS OF O_2H_2
FUNCTION TO BE INTEGRATED

~~SECRET~~

~~SECRET~~

critical mass and hydride density may be approximated. By reasoning similar to that of the last section, the following relation holds if the density of $OyH_{2.93}C_{1.08}O_{0.26}$ (R, M) is changed from ρ_0 to $\rho = \rho_0 + \Delta\rho$:

$$4\pi \int_0^{r_0} R(r) \frac{\rho_0}{M} \frac{\Delta\rho}{\rho_0} r^2 dr \approx \Delta V_c \left[R_u(r_0) \frac{\rho_u}{M_u} - R_0(r_0) \frac{\rho}{M} \right],$$

again R_u , ρ_u and M_u apply to Tu, r_0 is the initial core radius and ΔV_c is the change in critical volume V_c . This may be combined with

$$\frac{\Delta M_c}{M_c} = \frac{\Delta V_c}{V_c} + \frac{\Delta\rho}{\rho},$$

the fractional change of critical mass, to give

$$\frac{\Delta M_c}{M_c} \approx \frac{\Delta\rho}{\rho} \left[1 + \frac{3 \int_0^{r_0} R(r) r^2 dr}{r_0^3 \left(\frac{R_u(r_0)\rho_u}{\rho_0 M_u} - R(r_0) \right)} \right], \Delta\rho \ll \rho_0.$$

Inserting $R(r_0) = 91.5$ cents/mole, $\rho_0 = 7.35$ gm/cm³, $M = 255$, $R_u(r_0) = 13.1$ cents/mole, $\rho_u = 19.0$ gm/cm³, $M_u = 238$ and $r_0 = 7.8$ cm, this becomes

$$\frac{\Delta M_c}{M_c} \approx \frac{\Delta\rho}{\rho} (1 - 1.11 \times 10^{-4} \int_0^{r_0} R r^2 dr),$$

and graphical integration gives

$$\frac{\Delta M_c}{M_c} \approx -1.57 \frac{\Delta\rho}{\rho},$$

or $M_c \approx \text{const.} \rho^{-1.57}$.

This indicates a more rapid variation with density than is accepted for Oy in thick Tu temper.⁽⁸⁾ Although data for the Ni tamped hydride are too sketchy for a similar computation, more extreme variations with radius indicate an exponent even greater in absolute value than that given by the above computation.

⁽⁸⁾ W-Division Progress Report, LAMS-940, (7/21/49-8/20/49).

~~SECRET~~

END